Bulletin of the Geological Society of Malaysia, Volume 71, May 2021, pp. 159 - 183
DOI: https://doi.org/10.7186/bgsm71202114

Geothermal gradient and heat flow maps of offshore Malaysia: Some updates and observations

Mazlan Madon[1,2,*], John Jong[3]

[1] Malaysian Continental Shelf Project, National Security Council, Malaysia
[2] Department of Geology, Universiti Malaya, 50603 Kuala Lumpur, Malaysia
[3] JX Nippon Oil and Gas Exploration (Malaysia) Limited, Malaysia
* Corresponding author email address: mazlan.madon@gmail.com

Abstract: An update of the geothermal gradient and heat flow maps for offshore Malaysia based on oil and gas industry data is long overdue. In this article we present an update based on available data and information compiled from PETRONAS and operator archives. More than 600 new datapoints calculated from bottom-hole temperature (BHT) data from oil and gas wells were added to the compilation, along with 165 datapoints from heat flow probe measurements at the seabed in the deep-water areas off Sarawak and Sabah. The heat flow probe surveys also provided direct measurements of seabed sediment thermal conductivity. For the calculation of heat flows from the BHT-based temperature gradients, empirical relationships between sediment thermal conductivity and burial depth were derived from thermal conductivity measurements of core samples in oil/gas wells (in the Malay Basin) and from ODP and IODP drillholes (as analogues for Sarawak and Sabah basins). The results of this study further enhanced our insights into the similarities and differences between the various basins and their relationships to tectonic settings. The Malay Basin has relatively high geothermal gradients (average ~47 °C/km). Higher gradients in the basin centre are attributed to crustal thinning due to extension. The Sarawak Basin has similar above-average geothermal gradients (~45 °C/km), whereas the Baram Delta area and the Sabah Shelf have considerably lower gradients (~29 to ~34 °C/km). These differences are attributed to the underlying tectonic settings; the Sarawak Shelf, like the Malay Basin, is underlain by an extensional terrane, whereas the Sabah Basin and Baram Delta east of the West Baram Line are underlain by a former collisional margin (between Dangerous Grounds rifted terrane and Sabah). The deep-water areas off Sarawak and Sabah (North Luconia and Sabah Platform) show relatively high geothermal gradients overall, averaging 80 °C/km in North Luconia and 87 °C/km in the Sabah Platform. The higher heat flows in the deep-water areas are consistent with the region being underlain by extended continental terrane of the South China Sea margin. From the thermal conductivity models established in this study, the average heat flows are: Malay Basin (92 mW/m^2), Sarawak Shelf (95 mW/m^2) and Sabah Shelf (79 mW/m^2). In addition, the average heat flows for the deep-water areas are as follows: Sabah deep-water fold-thrust belt (66 mW/m^2), Sabah Trough (42 mW/m^2), Sabah Platform (63 mW/m^2) and North Luconia (60 mW/m^2).

Keywords: geothermal gradient, thermal conductivity, heat flow, Malaysia, temperature data

INTRODUCTION

Geothermal gradients are an important parameter in the analysis of sedimentary basins, particularly for the modelling of organic maturation and petroleum systems. It provides a starting point for the estimation of heat flow in a particular a region and is closely related to tectonic setting. The primary source for geothermal gradients at continental margins is temperature measurements in oil and gas wells. Much of those data, however, remained locked in oil company archives.

The offshore Tertiary sedimentary basins of Malaysia provide valuable information on the geothermal gradient of the Southeast Asian region. Unfortunately, large data gaps exist in the current geothermal gradient maps which were published in 1999. Figure 1 shows the geothermal gradient data for offshore Malaysia from Madon (1999), along with public domain data obtained from the Global Heat Flow Database (GHCG, 2013). An update is long overdue. In this article we present an updated geothermal gradient database for offshore Malaysia that incorporates previously unpublished information compiled from regional studies conducted by various oil and gas operators in Malaysia.

This is a progress report of an on-going effort to update the geothermal gradient and heat flow maps of Malaysia's offshore regions. Our objectives in this study were to review, verify and validate the geothermal data in a consistent manner to generate the updated maps. With this update, we also made some observations on the geothermal gradient, thermal conductivity and heat flow data and their geological implications.

GEOLOGICAL SETTING

The main Tertiary sedimentary basins of Malaysia are situated in three regions – offshore east of Peninsular Malaysia (namely the Malay and Penyu basins), offshore

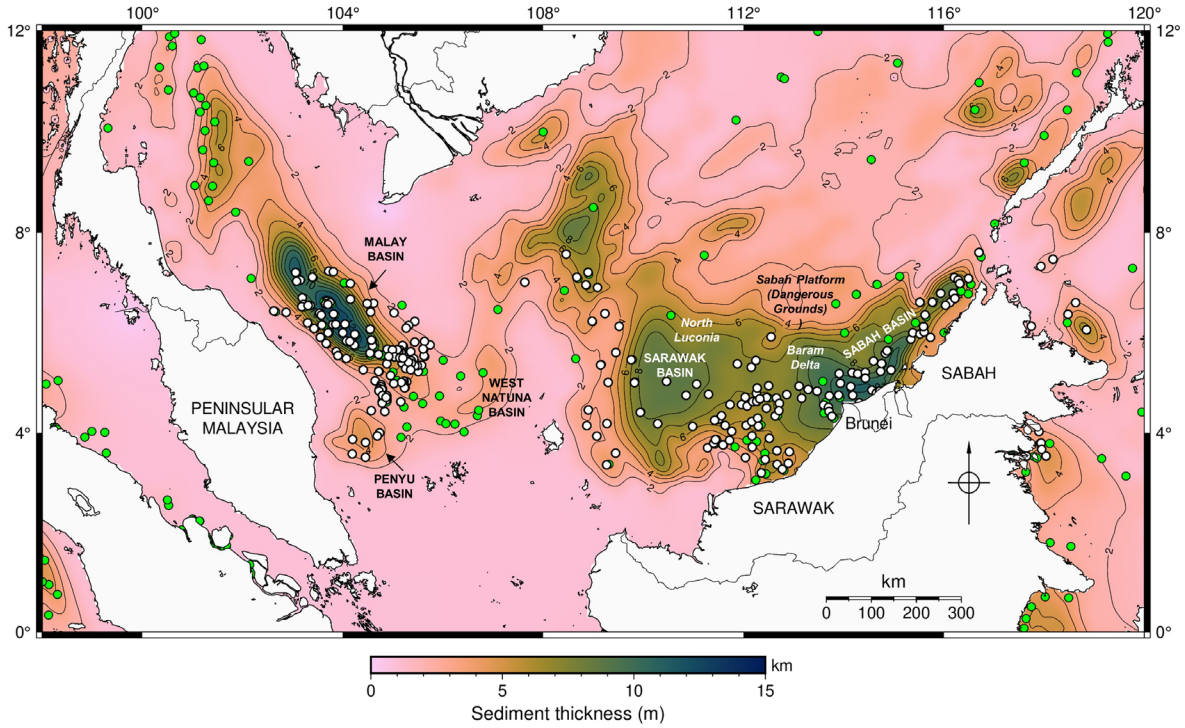

Figure 1: Map of offshore regions of Malaysia showing the sediment thickness in the three major basins (Malay, Sarawak and Sabah basins) based on GlobSed global grid (Straume *et al*., 2019) overlaid with geothermal gradient datapoints (white circles) from the PETRONAS map compiled by Madon (1999). The total number of datapoints in that compilation was 216 excluding those outside Malaysia's maritime boundaries but including some points from Brunei. Green circles represent data from the Global Heat Flow Database (GHCG, 2013).

Sarawak (Sarawak Basin) and offshore NW Sabah (Sabah Basin). The basins are filled with more than 12 km of sediments which range in age from at least late Eocene to Quaternary. The Malay and Penyu basins are extensional or strike-slip related basins developed on late Mesozoic continental crust (Madon *et al.*, 1999; Morley, 2002; Morley & Leong, 2008; Madon *et al*., 2019). The Sarawak and Sabah basins are continental margin basins which had a more complex history involving rifting, collision and subduction associated with the evolution of the eastern Sundaland margin and the South China Sea during the late Cretaceous to Tertiary (e.g., Taylor & Hayes, 1983; Hayes & Nissen, 2005; Pubelier & Morley, 2014; Hall & Breitfeld, 2017).

Whereas the Malay and Penyu basins are essentially rift-type intracontinental basins formed in continental crust underlying the broad Sunda Shelf, the Sarawak and Sabah basins are part of the greater NW Borneo basin system. The latter is underlain by attenuated continental crust that forms the southern rifted margin of the South China Sea marginal basin (Gozzard *et al.*, 2016), with which its tectonic history is closely interlinked (e.g., Hazebroek & Tan, 1993; Hutchison, 2004, 2010; Hutchison & Vijayan, 2010; Franke *et al.*, 2008, 2011). The various tectonic histories have resulted in contrasting sedimentary and geomorphological evolution of the three regions and, as this study shows, also resulted in differing geothermal and heat flow regimes.

DATA SOURCES

In Malaysia, data related to oil and gas are held by PETRONAS, the national oil company. The last geothermal gradient compilation was published in 1999 in PETRONAS's book, "Petroleum Geology and Resources of Malaysia", Chapter 5 (Madon, 1999). We have included as many datapoints as possible from the archives of PETRONAS, including data from wells drilled before 1999 but were not available previously and from wells drilled subsequently until 2017. In addition, we have also reviewed and included unpublished data from Shell and Esso that were made available to us during data room sessions.

To complement the Malaysian data and to fill the data gaps in neighbouring offshore areas, we also included data from the intervening areas in offshore Brunei, mainly from Sandal (1997), and in the Natuna region (Indonesia), mainly from the SEAPEX/IPA geothermal gradient map (Kenyon & Beddoes, 1977; Rutherford & Qureshi, 1981) as well as the relatively recent data from Budi & Miftahul (2014). Finally, we compared our data with the available Malaysian data in the Global Heat Flow Database maintained by the International Heat Flow Commission (IHFC) (http://ihfc-iugg.org/) (GHCG, 2013) in order to check their accuracy and identify potential errors. The distribution of the global data outside Malaysian waters are plotted as green circles in Figure 1.

Data corrections

Present-day geothermal gradients in sedimentary basins are usually estimated from measurements of formation temperatures in oil and gas wells. These are derived from bottom-hole temperatures (BHT) of the circulating drilling mud in oil/gas wells during logging runs or from formation-fluid temperatures recorded during repeat formation tests (RFTs), drill-stem tests (DSTs) and production tests (PTs). Barring any operational errors or instrument failures, temperatures measured during DSTs and PTs are generally considered to be the most reliable (Hermanrud *et al*., 1990, 1991; Peters & Nelson, 2009) and are generally accepted as valid without further correction. BHTs are generally lower than the true formation temperatures and must be corrected, using one of a number of correction techniques (e.g., Waples & Ramly, 1994; 2001). Based on their analysis of Malay Basin data, Waples & Ramly (1994) recommended that a standard correction of +16% be added to BHT-derived temperatures.

Malay and Penyu basins

Early estimates of the geothermal gradient in the Malay Basin were made by Matsubayashi & Uyeda (1979) based on BHTs in eight exploration wells. This was followed by the work of Wan Ismail (1984a, b) who used a more extensive data base of 49 wells, including measurements of thermal conductivity of over 650 core samples from the Malay Basin. In that study, temperature gradients were calculated from BHTs corrected using the standard method (Evans & Coleman, 1974). Wan Ismail (1990) expanded the database to include PT data from 23 wells. This body of work on Malay Basin formed the basis for an MSc thesis (Wan Ismail, 1993), a large part of which remained unpublished. The Malay Basin database was updated by Mohd Firdaus (1994) who obtained more measurements of thermal conductivity in core samples, not just from Malay Basin but also from the Sarawak and Sabah basins. Subsequently, more datapoints compiled from well completion logs and well test results were added to this database (Madon, 1999). The results up to that time showed that the geothermal gradients in the Malay Basin range between 45 and 60 °C/km, with several wells in the basin centre having values >70 °C/km. We have included all these previous datasets in our compilation and added new datapoints from wells that have BHT data. For the calculation of geothermal gradients in the Malay and Penyu basins, where the wells in our compilation were drilled in water depths of between 33 and 85 m (average 65 m), a constant seabed temperature of 24 °C (75 °F) was assumed.

Sarawak and Sabah basins

In offshore Sarawak and Sabah, the data were compiled from unpublished regional studies, such as those by Shell (e.g., Jong & Ho, 2000; Scherer *et al.*, 2000), as well as from well summary reports for the post-2000 wells, with input from our ex-colleagues in Shell and PETRONAS. As mentioned, since raw BHTs obtained from wireline logs are generally cooler than true formation temperatures, corrections have been applied. In the dataset compiled by Shell, it was noted that the BHT data were corrected by either the CTRM (Compensated Time Ratio Method; Burri & Miroschedji, 1976), or the CTCYM (Corrected Temperature by the Cylinder Method; Brandenburg, 1994) methods. Both these methodologies were developed in-house by Shell and are variants of the Horner plot correction procedure. Wells drilled by other operators were generally corrected by the Horner plot method, especially when multiple BHT measurements from successive logging runs were available. Geothermal gradients were then calculated based on the corrected BHTs.

It is important to point out that the value of seabed temperature used in the calculation of geothermal gradient can have a significant impact on the results, especially if the water depth range is large. In the Sarawak and Sabah basins, wells were drilled in water depths ranging from 0 to almost 2000 m. The seabed temperature is therefore unlikely to be constant. Seabed temperature data for NW Borneo margin compiled by Shell (Jong & Ho, 2000) show that seabed temperature decreases exponentially with increasing water depth, with temperatures dipping below 10 °C at a water depth of about 375 m (Figure 2A). On the shelf, where water depths are less than 200 m, seabed temperatures seem to vary almost linearly between about 30 °C and 14.5 °C (Figure 2B). It is noted that in our compilation 95% of the wells in offshore Sarawak and Sabah were drilled in water depths of less than 375 m. If we consider only the seabed temperatures down to 375 m, the mean seabed temperature is 23.6 °C (standard deviation of 5.51 °C). Thus, it seems reasonable to assume an average seabed temperature of 24 °C for shallow water wells, as was done in the Malay Basin. For the Sarawak and Sabah basins, however, due to the large range in water depths, using a constant seabed temperature may have a significant effect on the calculated geothermal gradients. Based on our review, the seabed temperature data in Figure 2A have been used as a guide to determine the appropriate seabed temperatures in the calculation of geothermal gradients.

A major addition to the current geothermal gradient database are numbers compiled for the first time from the deep-water areas of Sarawak (North Luconia) and Sabah (Sabah Platform or Dangerous Grounds) (Figure 3). This was made possible by the availability of direct measurements of heat flow at the seabed using marine heat-flow probes (see, e.g., Nagihara *et al.*, 2002 for a summary of the technique). The marine heat flow surveys were carried out between 2002 and 2013 by PETRONAS and several other oil companies who operated in their deep-water acreages. None of the studies have been published except some aspects of heat flow by JX Nippon in the Sabah Trough (McGiveron & Jong, 2018). There was also some information from deep-water Brunei (Zielinski *et al.*, 2007), to which we do not have access. Neither of these published studies include specific details

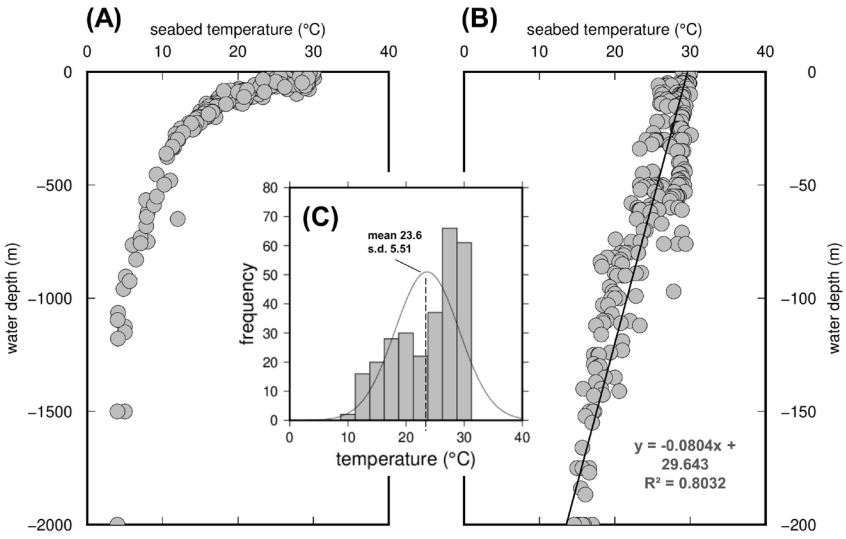

Figure 2: Seabed temperature data for NW Borneo margin compiled by Shell (Jong & Ho, 2000). (A) Seabed temperatures in water depth down to 2000 m, showing exponential decrease in temperature with increasing water depth. (B) A subset of the data in A showing only data from 0 to 200 m (shelf area). The temperature change with depth from 30 °C to 14.5 °C can be approximated by a linear regression line as indicated. (C) Histogram of seabed temperatures from the dataset in A within the depth range of 0 to 375 m shows a mean of 23.6 °C and standard deviation (s.d.) of 5.51. Note that the higher frequencies in the upper range of temperatures is due to more wells drilled in shallow water (hence higher seabed temperatures).

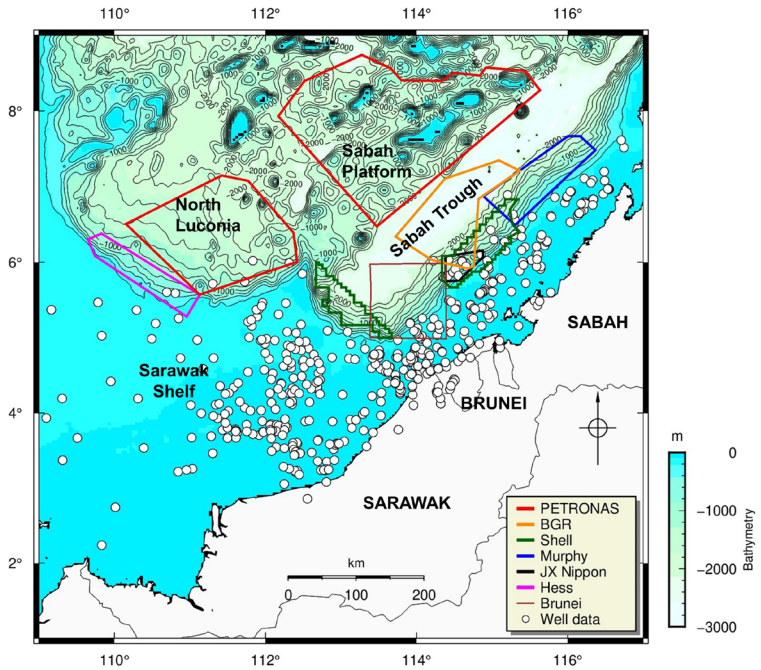

Figure 3: Marine heat flow surveys carried out by various oil companies (2002 – 2013) and research institutions (BGR, 1987-88) in the deep-water areas, which include North Luconia, Sabah Platform and Sabah Trough. This dataset complements the data available on the shelf (white circles on blue background) and onshore regions collected through years of oil/gas exploration since the early 1950s. Bathymetric contours at 200 m intervals start at -200 m (shelf-slope break) down to -2000 m water depth.

of the geothermal gradient or heat flow data. Besides the oil company surveys, marine heat flow surveys were undertaken in the Sabah Trough by the German Federal Institute for Geosciences and Natural Resource (BGR) during its 1987-88 cruises. The results were also included in our compilation.

All the heat-flow probe surveys mentioned above, which were largely in unexplored and undrilled deep-water regions, provided important information that complements the BHT-derived data in the shelf areas, as well as the proximal deep-water areas of Sarawak and Sabah. In total, these heat flow surveys contributed 165 additional datapoints to our database. With this dataset, we now have in our compilation a total of 835 datapoints from the three major Tertiary basins of Malaysia.

GEOTHERMAL GRADIENT RESULTS

Malay and Penyu basins

A map of geothermal gradients of the Malay and Penyu basins is shown in Figure 4. We can see that most of the geothermal gradients in the Malay Basin are above 35 °C/km, with some reaching 75 °C/km. Some lower values are observed in the Penyu Basin. It is worth pointing out that since the datapoints were based on oil/gas wells, they are located on structural anomalies, many of which are hydrocarbon-filled structural traps. As no wells have been drilled in the synclinal areas between the structures, the datapoints may be considered as "anomalies" due to "biased" sampling of geothermal gradients. Also, the high geothermal gradients on these structural highs may be as

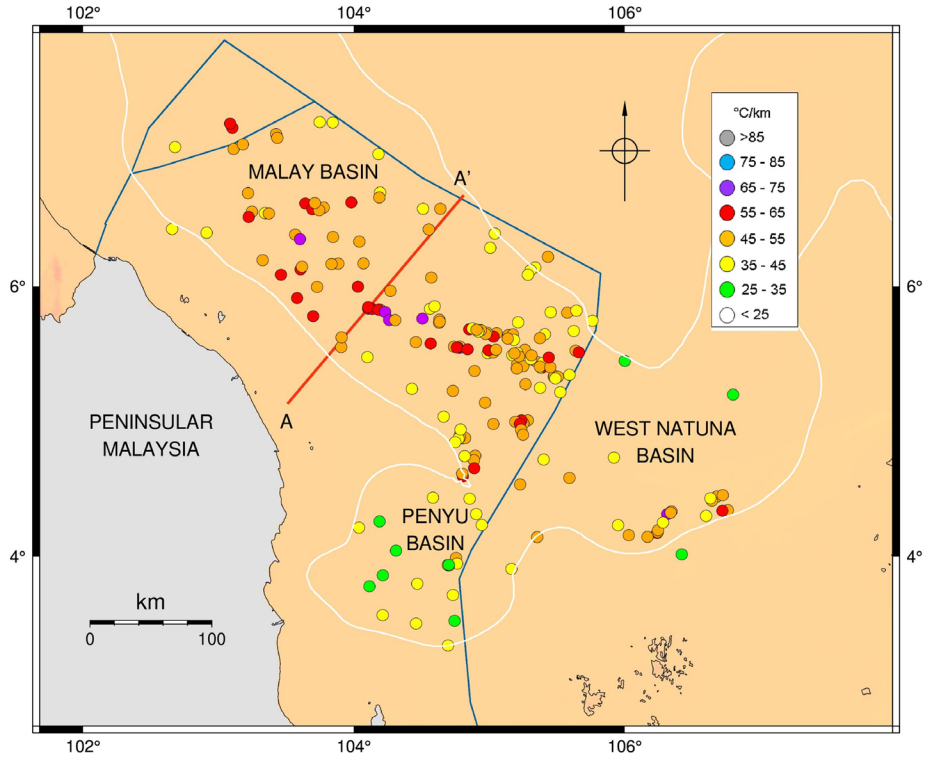

Figure 4: Geothermal gradients in the Malay and Penyu basins, whose outline is indicated by the sediment thickness contours at 2000 m. Line AA' represents the location of a NE-SW oriented 2D plane (shown in Figure 5) onto which the temperature gradient points have been projected, in order to represent a 2D profile of the geothermal gradient across the basin. Sediment thickness contours were extracted from GlobSed grid (Straume *et al*., 2019).

expected since they could have been influenced by migration of hot hydrocarbon-bearing fluids from deep sources (kitchen areas). The close link between hydrocarbon pools and high geothermal gradients has long been established in some basins (Majorowicz *et al*., 1986; Jones & Majorowicz, 1987; Zielinski *et al.*, 2007; Tang *et al.*, 2014). It is also noted that the high values of geothermal gradient (>35 °C/km) occur mainly in the central basin trough, which approximately coincides with the 4000 m sediment thickness contour.

The geothermal gradient can be displayed in two dimensions by projecting the data onto a 2D plane located along a profile across the central Malay Basin (Line AA' in Figure 4). The profile clearly shows that lower geothermal gradient values mainly occur on the basin flanks whereas the number of high geothermal gradient values gradually rise towards the basin centre. The envelope of maximum geothermal gradient (approximated by the dashed line in Figure 5) is almost a mirror image of the top of pre-Tertiary basement identified on the interpreted seismic section RC93-13 (lower panel in Figure 5). The apparent correlation between geothermal gradient and basement depth is likely to be related to crustal thinning beneath the basin as a result of basin extension. Due to isostasy, the top of basement is deepest and the sediment fill thickest where the underlying crust is thinnest. Gravity models have shown that the crust beneath the basin had been thinned by at least a (β) factor of 2.3 (Madon & Watts, 1998). Where the crust is thinner beneath the basin centre, lithospheric mantle is shallower and thus causing the higher heat flow and geothermal gradient.

The data for the Penyu Basin has been updated based on recently published information (Madon *et al.*, 2019). They show some low values (< 35 °C/km) compared to those of the Malay Basin. The much smaller dataset for the Penyu Basin is not sufficient to define any patterns in geothermal gradient. Like the Malay Basin, the Penyu Basin is also underlain by thinned crust (β=2) as indicated by gravity modelling (Madon & Watts, 1998). The lower geothermal gradients overall, however, probably indicate absence of major hydrocarbon accumulations and the lack of hot fluids circulating or migrating within the basin. It is noted that geothermal gradients on the Tenggol Arch between the Malay Basin and Penyu Basin are slightly higher, ranging from 35 to 55 °C/km, with one point up to 65 °C/km.

Sarawak and Sabah basins

The 1999 geothermal gradient map of offshore Sarawak and Sabah (Madon, 1999) was based on a compilation by Occidental Oil Co. (Oxy) in 1989 and consisted of approximately 250 datapoints. We have now updated the database with more than 500 points compiled from the archives of PETRONAS and Shell (Figure 6). Also included are datapoints on the Brunei Shelf (Sandal, 1997), which show strong similarities with the Sarawak side of the Baram Delta Province as well as the Sabah Shelf. Geothermal gradients in the Baram Delta are generally 35 °C/km or less (green points, Figure 6) whereas on the Sarawak Shelf the gradients are mainly >35 °C/km (yellow and orange points, Figure 6). It should be pointed out also, as for the Malay Basin, there may have been a biased sampling of

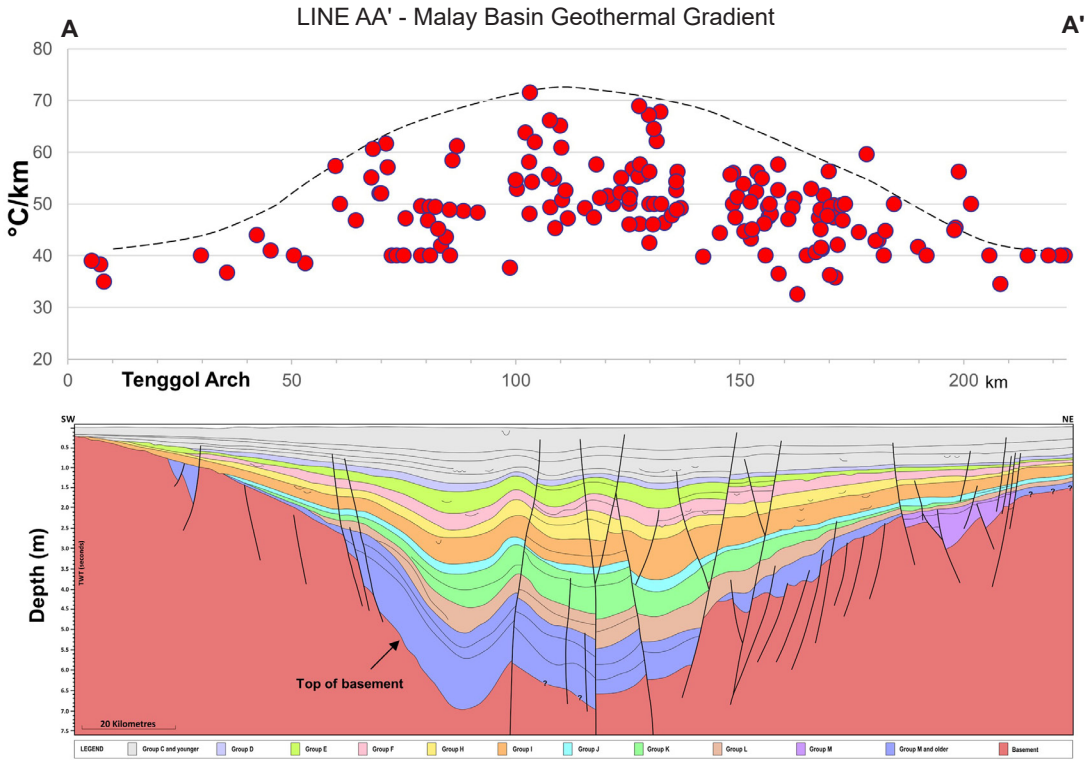

Figure5: Geothermal gradient profile Line AA' across the Malay Basin. Upper panel shows the geothermal gradient data points projected onto the 2D plane AA' (see Figure 4 for location). Lower panel is an interpreted seismic section along the profile, based on regional seismic line RC93-13 (redrawn from Yu & Yap, 2019). Tertiary sediments filling the basin are colour-coded. High geothermal gradients seem to correlate with thick sediment fill at the basin centre where the crust is probably thinnest.

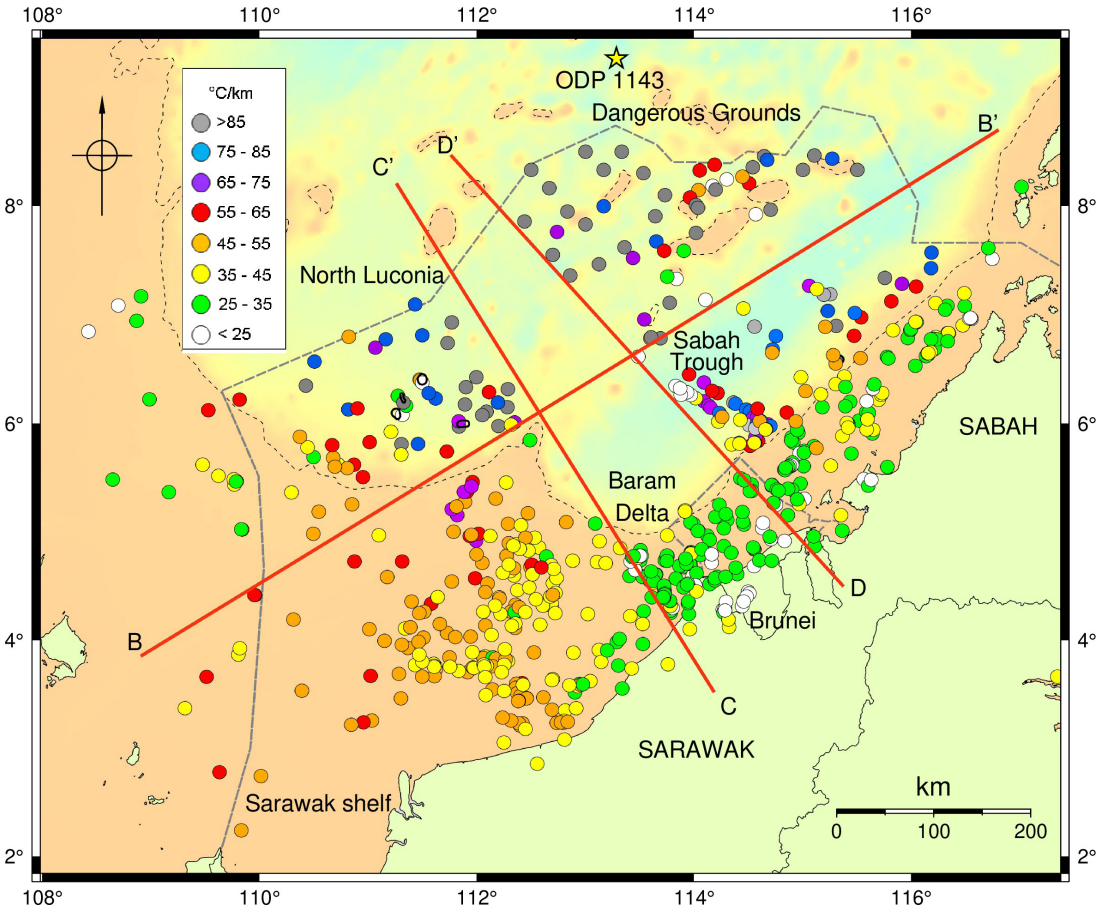

Figure 6: Geothermal gradient points in the Sarawak and Sabah basins compiled in the current update. Lines BB', CC', and DD' are the location of 2D planes onto which geothermal gradient datapoints are projected, as shown in Figures 7 and 9. Profile BB' includes only data points south and east of line BB' excluding those beyond the shelf-break in the Sabah Trough. Profile CC' includes only data points located west of line CC', while Profile DD' includes only data points east of line DD'.

geothermal gradients in Sabah and Sarawak, since the wells commonly targeted structural highs and, as often the case in the Baram Delta, are located near growth faults where sand-shale ratios (and therefore fluid transmissibility) are typically higher. Thus, in places close to growth fault structures, heat transfer by fluid flow tends to increase the temperatures at any given depth compared to areas down-dip from the faults. Furthermore, higher sedimentation rates away from growth faults tend to depress the temperatures at any given depth, resulting in lower geothermal gradients. Similar trends linked to sedimentation rates and fluid flow effects have been observed in the US Gulf Coast (e.g., Border *et al*., 1985).

In Figure 6, a line of contrast in geothermal gradients roughly coincides with the 200 m isobath that marks the NW-trending shelf-slope break at the western limit of the Sabah Trough. This feature also represents the approximate position of the West Baram Line (WBL) which is often interpreted as a major tectonic discontinuity of regional geological significance in the NW Borneo margin (e.g., Cullen, 2014; Kessler & Jong, 2016). As indicated by the contrasting colour-coded datapoints in Figure 6, the Sarawak Shelf is characterised by relatively higher geothermal gradients (with values similar to the Malay Basin) whereas the deep-water areas (North Luconia, Dangerous Grounds and Sabah Trough) generally have higher geothermal gradients compared to the shelf areas.

As was done for the Malay Basin, the geothermal gradient data were projected onto 2D planes to show their distribution along and across the margin. For this purpose, three synthetic 2D profiles were created as shown on the map in Figure 6; one profile along strike (BB') sub-parallel to the Sarawak and Sabah coastline extending for 1000 km, and two NW-SE profiles perpendicular to the coastline, one across the Sarawak margin (CC'), and the other across the Sabah margin (DD'). It should be pointed out that these are not actual profiles but are merely 2D planes onto which the datapoints are projected. In Figure 7, for example, profile BB' represents the projection of all datapoints that are located landward of the 200 m isobath and to the south and east of line BB'. In other words, the plot in Figure 7 represents only those points on the Sarawak Shelf, Baram Delta and Sabah Shelf; datapoints in the Sabah Trough are excluded. We can see from the profile, as indicated also by the map in Figure 6, that generally the geothermal gradients on the Sarawak Shelf are significantly higher (average 45.9 °C/km) than those in the adjacent Baram Delta area (average 28.9 °C/km). As mentioned, the boundary between an area of generally high geothermal gradient (Sarawak Shelf) and an area of low geothermal gradient (Baram Delta) is represented by the NW-trending 200 m isobath at the shelf-slope break facing the Sabah Trough, which is also the approximate location of the WBL.

The artificial profiles BB', CC' and DD' in Figure 6 effectively subdivides the margin into several quadrants and their constituent datapoints. Starting from the southwest, they are Sarawak Shelf, Baram Delta, Sabah Shelf, and the deep-water areas of North Luconia and Sabah Platform in Sarawak and Sabah, respectively. Figure 8 shows the histograms and statistics of the geothermal gradient datapoints in the individual quadrants, along with those of the Malay and Penyu basins. The average geothermal gradient for each quadrant (region) is compared with estimates from previous works (Table 1).

The similarities and differences in geothermal gradients between the basins may be related to their tectonic settings. The Sarawak Basin is underlain by extensional terranes characterised by Eocene-Oligocene half-grabens in the pre-Oligocene (pre-Cycle I) crust, as has been documented particularly in the Half-Graben and Tatau provinces on the southwestern Sarawak Shelf (Madon & Redzuan, 1999; Jabbar *et al.*, 2015). The geothermal gradient is therefore expected to be relatively high, although slightly lower than that of the Malay Basin (compare Figures 8A and 8F). The Baram Delta, as are many deltaic basins, is characterised by rapid sedimentation rate and consequently thick sediment accumulation. In some basins, it has been shown that geothermal gradients tend to be lower in areas of rapid sedimentation due in part to the thermal blanketing effect of "cool" sediments inhibiting heat transfer to the surface (Karner, 1991). Studies have shown that a pile of thick sediments in basins retards the heat flow to the surface, resulting in lower geothermal gradients (e.g., Kim *et al*., 2020). Like the Baram Delta, the Sabah Shelf is underlain by a huge thickness of sediments and therefore shows similar but slightly higher geothermal gradient values, especially in the outboard areas towards the Sabah Trough.

Figure 9 shows the projected geothermal gradient data along Lines CC' and DD' (see Figure 6 for location) which represent the dip profiles of geothermal gradient across the Sarawak and Sabah margin, respectively. The data clearly

Table 1: Summary of geothermal gradients determined in this study, compared with previous works. Deep-water areas are separated into Sabah deep-water fold-thrust belt (DWFTB), Sabah Trough, Sabah Platform (or Dangerous Grounds) and Sarawak Deep-water (or North Luconia). n.a. – not available in previous studies.

Basin (region)	Rutherford & Qureshi (1981)	Mohd Firdaus (1994)	This study
Malay Basin	44.7	51.8	47.6
Sarawak Shelf	42.8	43.3	45.2
Baram Delta	n.a.	n.a.	28.7
Sabah Shelf	28.2	30.5	31.7
Sabah DWFTB	n.a.	n.a.	63.8
Sabah Trough	n.a.	n.a.	45.7
Sabah Platform	n.a.	n.a.	87.0
Sarawak Deep-water	n.a.	n.a.	80.1

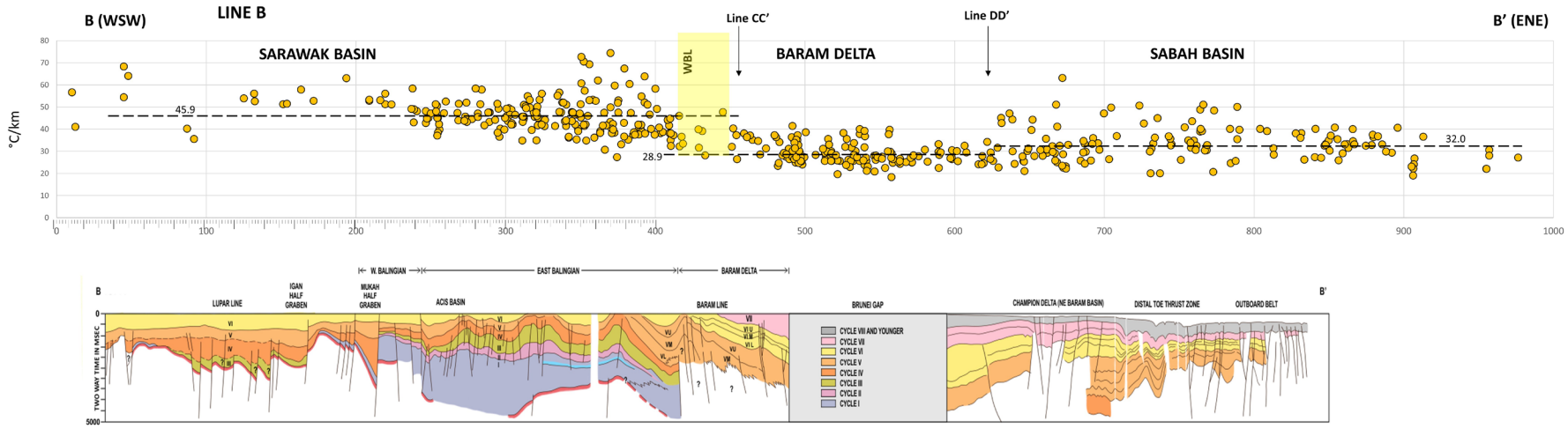

Figure 7: Top panel is a 2D profile BB' (see location in Figure 6) onto which geothermal gradient datapoints on the south side of the line are projected, representing only the geothermal gradient of the shelf areas (water depth less than 200 m). Horizontal dashed lines represent the average geothermal gradient for the three segments of the shelf: Sarawak (45.9), Baram Delta (28.9) and Sabah (32.0). The lower panel is a composite profile along strike of the Sarawak and Sabah margin showing the main structural features, in particular the West Baram Line. Interpreted seismic profile redrawn from Rice-Oxley (1992) and Lee (2000).

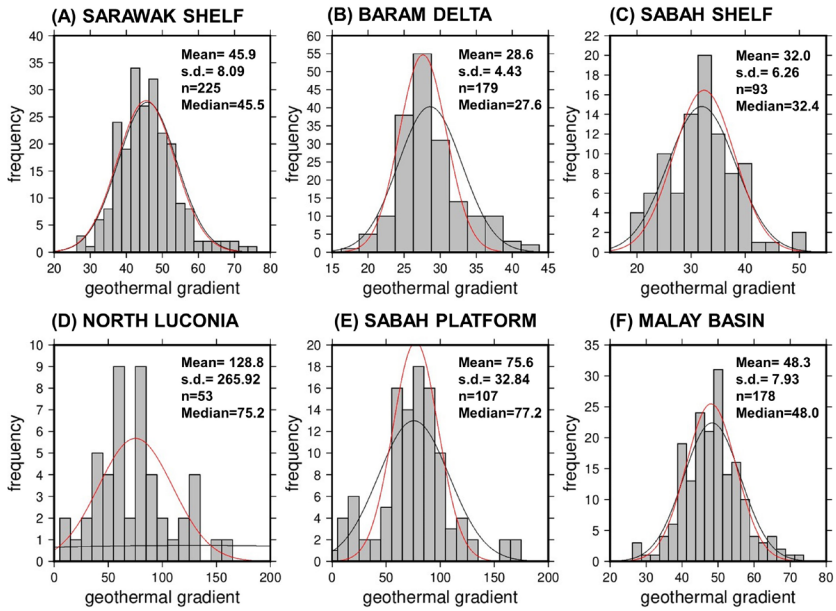

Figure 8: Histograms of geothermal gradient points plotted in Figures 4 and 6 for the different segments of the Malaysian offshore regions, summarised by the corresponding statistics. (A) Sarawak Shelf. (B) Baram Delta, including Sarawak, Brunei and Sabah parts. (C) Sabah Shelf. (D) North Luconia (deep-water Sarawak). (E) Sabah Platform (Dangerous Grounds, deep-water Sabah). (F) Malay Basin. Except for regions D and E, all datapoints are located landward of the 200 m isobath. The black curves in all the graphs represent the calculated normal distribution with the stated mean and standard deviation, while the red curves represent the normal distribution calculated based on the Median Absolute Deviation (MAD) with the standard deviation given by 1.4826*MAD. Note that in (D) where the distribution is more erratic, MAD is a better estimator of the central location of the distribution (i.e. median).

show higher geothermal gradients in the deep-water areas of both Sarawak (North Luconia) and Sabah (Sabah Platform) compared to the adjacent shelf areas. There is significant scatter, however, in the geothermal gradient values from point to point due to localised effects of hydrothermal activity and pore-water advection, as reported in the marine survey report (Zielinski & Zielinski, 2003).

Marine heat flow surveys

Heat flow surveys using heat flow probes in the deep-water areas off Sarawak and Sabah (in water depths down to >2900 m) have been carried out by oil companies including PETRONAS since 2002. These surveys covered much of North Luconia, Sabah Platform (Dangerous Grounds) and Sabah Trough (Figure 3), and provide critical geothermic information in the deep-water areas in order to complement the BHT data from the shelf areas. In 2002 Hess surveyed the northern slopes of the Sarawak margin where a number of exploration wells were subsequently drilled. In 2003 Shell carried out heat flow surveys in several deep-water blocks in the Sabah Trough: Block E at the north-eastern edge of Central Luconia facing the Sabah Trough and Blocks G and J in the deep-water fold-thrust belt (DWFTB) (Figure 3). Murphy surveyed the north-eastern part of the DWFTB in 2005 and in 2013 JX Nippon collected heat flow and geothermal gradient data in the south-western part, close to Brunei. Some aspects of the JX Nippon survey have been published by McGiveron & Jong (2018). These two surveys by the oil industry complement the heat flow measurements by BGR taken during its research cruises SO-49 (1987) and SO-58 (1988) in the central parts of the Sabah Trough as part of its research collaborations with PETRONAS during the late 1980s (e.g., Hinz *et al.*, 1989).

Also, in 2003 PETRONAS commissioned a major heat flow survey further outboard in the Sabah Platform and North Luconia areas, covering large parts of the deep-water areas of Sarawak and Sabah (Zielinski & Zielinski, 2003). Altogether, there were 92 sites in water depths of 800 to >2000 m, where *in situ* measurements of geothermal gradient and heat flow were taken simultaneously using thermistors attached to gravity core barrels. Thermal conductivity was also measured on sediment cores on board the ship. All the measurements, 41 for Sarawak and 51 for Sabah, were reported as valid measurements, including several anomalously high values of temperature gradient and heat flow (> 290 °C/km, and correspondingly > 230 mW/m^2) with one particular site registering 1900 °C/km. Similar high readings were recorded in the Brunei margin where Zielinski *et al*. (2007) reported an abnormal heat flow value of 600 mW/m^2 associated with a "mega-seep" through a submarine mud volcano.

In Figure 9A, geothermal gradients start to increase dramatically seaward of the shelf-slope break into North Luconia. The highly variable geothermal gradient in the deep-water areas is clearly observed along selected bathymetric profiles shown in Figure 10. Some profiles cross prominent sea-floor features that coincide with structural highs in the subsurface. Some of those highs were the target of oil exploration and have been drilled into. Profiles A and B cross the shelf-slope break and pass through exploration well locations G2-1, Lanjak-1, and Paus-1 where prominent bathymetric highs show relatively lower geothermal gradients compared to other locations along the same profiles (Figure 10A, B). According to the survey report (Zielinski & Zielinski, 2003), the abnormally high readings in offshore Sarawak were related to a diapir-like subsurface structure that underlies a positive seafloor feature. That feature is

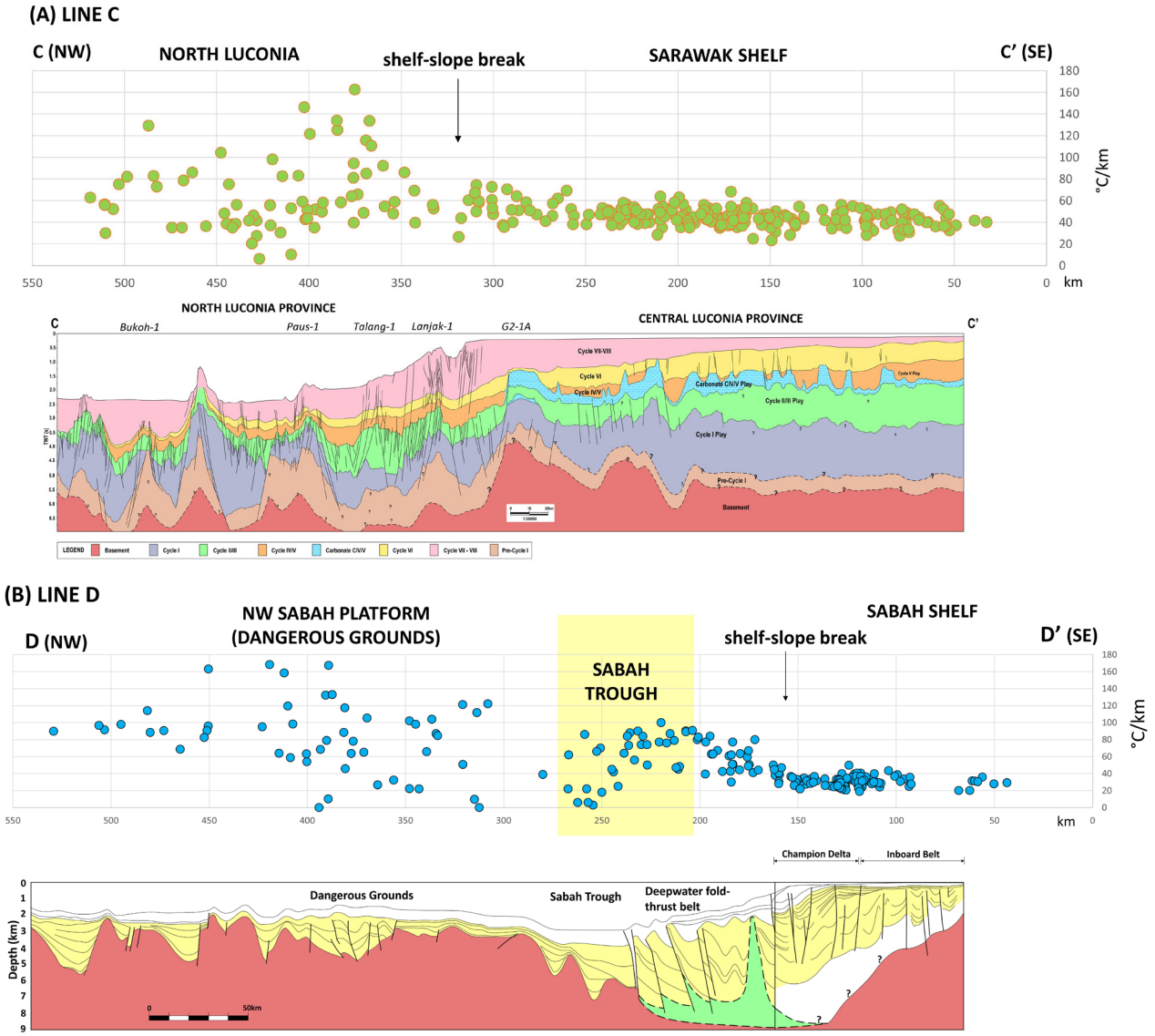

Figure 9: Geothermal gradient datapoints projected onto 2D profiles (A) Line CC' and (B) Line DD' (see Figure 6 for locations). For CC' only points to the west of Line C are projected, whereas for DD' only points to the east of Line D are projected. The positions of the shelf-slope break and the Sabah Trough are indicated for reference. The plots show significant scatter but overall higher geothermal gradients in the deep-water areas of North Luconia and Dangerous Grounds. The interpreted seismic profiles are based on (A) Iyer (2019) and (B) Yan & Liu (2004), with additional information on the Sabah Shelf from an unpublished Shell report (Lee, 2000). In (B) pink is pre-rift basement, yellow and white are sediment, and green is mobile shale.

clearly identifiable on Profiles C and D (Figure 10C and D, respectively). Profile C crosses three sea-floor features aligned in a NE-SW trend on the slopes of North Luconia. The most distal of those features is identified as the one that registered the anomalous geothermal gradient of 1900 °C/km. Profile D runs east-west and intersects Profile C exactly on the crest of that structure (see the map in Figure 10E). We can see that along Profiles C and D high geothermal gradients are associated with that particular sea-floor feature, a sketch of which is shown in Figure 10F.

In the Sabah Basin, it is observed in Figure 9B that geothermal gradients start to increase significantly seaward of the shelf-slope break into the Sabah Trough towards the distal (seaward) end of the Deep-water Fold-Thrust Belt. Bathymetric profiles in Figures 10G, H, and I also show, as in Figure 9B, significant scatter in the geothermal gradients across the Sabah Platform. They also indicate that not all bathymetric features are associated with high geothermal gradients. Two prominent seamounts in the middle of the Sabah Trough show contrasting geothermal gradient values – the northern one (Figure 10G) has relatively high gradients whereas the southern one (Figure 10I) has abnormally low gradients. High gradients overall in the Sabah Trough are indicated in Profile I (Figure 10H). Hence, while anomalously

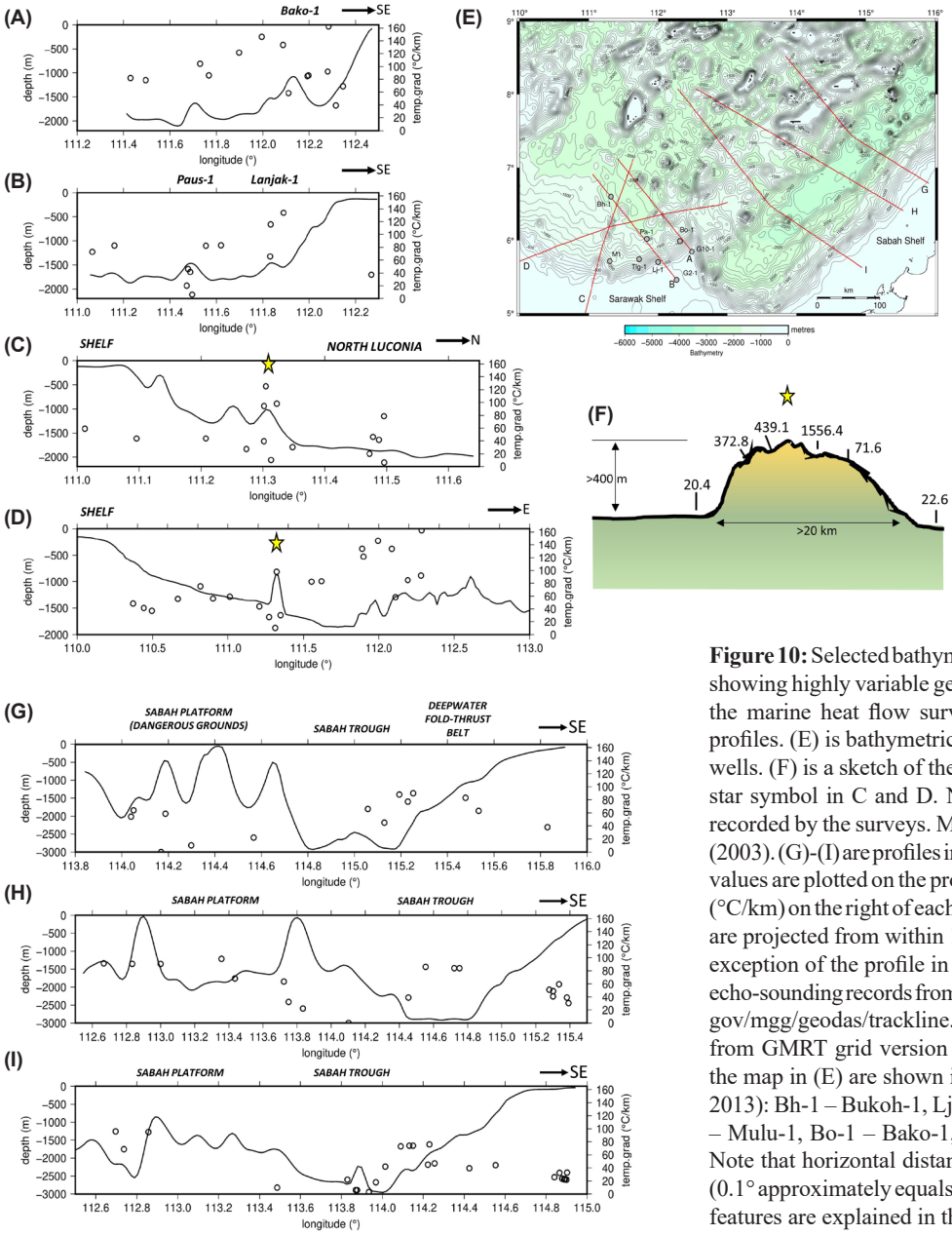

Figure 10: Selected bathymetric profiles across the study area, showing highly variable geothermal gradient recorded during the marine heat flow surveys. (A)-(D) are Sarawak Basin profiles. (E) is bathymetric map with location of profiles and wells. (F) is a sketch of the sea-floor feature identified by the star symbol in C and D. Numbers are heat flow in mW/m^2 recorded by the surveys. Modified from Zielinski & Zielinski (2003). (G)-(I) are profiles in Sabah Basin. Geothermal gradient values are plotted on the profiles as open circles, with the scale (°C/km) on the right of each plot. The geothermal gradient data are projected from within 10-20 km of each profile. With the exception of the profile in B, which is based on single-beam echo-sounding records from NCEI database (https://ngdc.noaa.gov/mgg/geodas/trackline.html), all profiles were extracted from GMRT grid version 3.8 (Ryan *et al*., 2009). Wells on the map in (E) are shown in grey circles (after Madon *et al*., 2013): Bh-1 – Bukoh-1, Lj-1 - Lanjak-1, Pa-1 - Paus-1, Mu-1 – Mulu-1, Bo-1 – Bako-1, Tlg-1 – Talang-1, G2-1, G10-1). Note that horizontal distance is plotted in degrees longitude (0.1° approximately equals 11 km). The profiles and their main features are explained in the text.

high geothermal gradients may be caused by hydrothermal activity, the low readings (<40 mKm^{-1})[1] at some sea-floor features in both Sarawak and Sabah deep-water areas may be due to pore-water advection in the seabed sediments. It should be mentioned that the origin of the Sabah Trough seamounts, which rise to more than 1.2 km above the sea floor, is uncertain. Franke *et al.* (2008) suggested that these conical features might be volcanoes, while Hutchison (2010) interpreted them as drowned Miocene carbonate reefs.

The presence of numerous deep-seated faults in the Dangerous Grounds and North Luconia rifted terranes (e.g., Hutchison & Vijayan, 2010; Savva *et al*., 2014) may have aided fluid circulation and heat transfer in the crust of this region. The variation in heat flow or geothermal gradient in the deep-water areas may also have been caused by the occurrence of gas/hydrates and/or other extraordinary sediment composition, bottom-water temperature seasonality, hydrothermal processes or sediment disturbances caused by

[1] The temperature gradient is measured in mKm^{-1} because the core length over which it is measured is only 4 m. It is assumed that the same constant surface temperature gradient extends several km downwards.

major sediment debris flow events. Abnormally high values of geothermal gradient (80-90 °C/km and even greater than 290 °C/km in places) were observed in the Sabah deep-water fold-thrust belt, on the slopes of North Luconia and in the deep-water off Baram Delta of Brunei. Some of these have been shown to be caused by hydrothermal activities associated with fluid escape pipes and mud volcanoes (McGiveron & Jong, 2018; Zielinski & Zielinski 2003, Zielinski *et al*., 2007). Zielinski *et al.* (2007) reported simultaneous heat flow measurements and extensive geochemical coring at 186 sites on the Brunei margin which indicate an area of mean heat flow of 84 mW/m^2 on the upper slope and an area of average heat flow of 59 mW/m^2 immediately seaward of the ~1000 m isobath. These values are similar to the heat flow values recorded by JX Nippon in the adjacent area along strike of the margin, with an average heat flow of 58 mW/m^2 and average geothermal gradient 66.5 °C/km (McGiveron & Jong, 2018).

Putting aside these abnormal local seabed conditions, variation in the heat flow and geothermal gradients, as indicated by the standard deviations, is low to moderate (Table 2). Overall, the mean geothermal gradient for the deep-water areas is quite similar: 80.1 °C/km for Sarawak (North Luconia) and 83.6 °C/km for Sabah Platform (Dangerous Grounds). The average heat flow for both areas is essentially the same, at around 60 mW/m^2. In addition, the thermal conductivity measurements seem to be consistent (an average of 1.025 Wm^{-1}K^{-1} over the entire deep-water region) and provide a good dataset for the calculation of heat flow. Table 2 summarises the statistics of the geothermic parameters from all the marine heat flow surveys.

CONTOURED GEOTHERMAL GRADIENT MAPS

From the newly compiled database of geothermal gradients shown in Figures 4 and 6, we generated contoured maps for Malay and Penyu basins (offshore Peninsular Malaysia) and for Sarawak and Sabah Basins (NW Borneo margin). To minimise contouring artefacts, it is desirable to have some "control points" beyond the region covered by datapoints. In Figure 5 it was observed that the geothermal

Table 2: Summary of thermal conductivity, heat flow and geothermal gradient measurements conducted in the deep-water areas off Sabah and Sarawak during the period 1987 to 2013, based on unpublished reports held by PETRONAS. K- conductivity, G – geothermal gradient, HF – heat flow. Numbers in brackets are standard deviation. Water depth is given as range from shallowest to deepest. K, G and HF values are quoted as mean and standard deviation. Average of thermal conductivity for the entire deep-water area is 1.025 Wm^{-1}K^{-1}.

SURVEY	BGR (1987/1988) - SABAH	HESS (2002) - SARAWAK	SHELL (2003) - SARAWAK	SHELL (2003) - SABAH	PETRONAS (2003) - SARAWAK	PETRONAS (2003) - SABAH	MURPHY (2005) - SABAH	JXNIPPON (2013) - SABAH
No. of stations	32	12	24	60	41	51	11	18
Water depth range (m)	838-2914	449-1178	447-1872	149-1643	923-2058	910-2272	585-1949	144-1480
K (Wm^{-1} K^{-1})	0.906 (0.092)	0.998 (0.081)	0.790 (0.059)	0.786 (0.072)	0.753 (0.021)	0.724 (0.029)	0.818 (0.0556)	0.924 (0.139)
G (mKm^{-1})	62.3 (26.3)	54.5 (11.4)	109.4 (36.3)	109.4 (53.2)	80.1 (38.0)	83.6 (41.3)	74.7 (11.97)	67.1 (21.6)
HF (mWm^{-2})	55.2 (22.8)	54.4 (13.1)	86.3 (130.4)	89.3 (49.9)	60.2 (28.7)	60.6 (30.5)	60.5 (6.85)	58.0 (17.72)

Notes:

The temperature gradient is measured in mKm^{-1} because the core length over which it is measured is only 4 m. It is assumed that the same constant surface temperature gradient extends several km downwards.

For Sarawak and Sabah data by Shell and PETRONAS, a small number of "highly anomalous" points (1-4 in each area) with G > 200 mKm^{-1} were excluded in the calculation of the average.

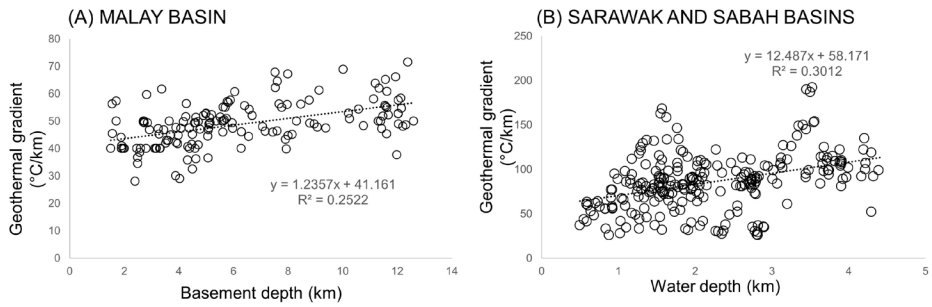

Figure 11: Correlations between geothermal gradient and (A) basement depth in the Malay Basin and (B) water depth (bathymetry) in the deep-water areas offshore Sarawak and Sabah.

gradients seem to mimic the shape of the sedimentary basin, whereby higher values of geothermal gradient occur above the basin centre where the top of pre-Tertiary basement is deepest. This relationship may be quantified by plotting the geothermal gradient at each well location against the corresponding depth to pre-Tertiary basement extracted from the basement depth map of the Malay Basin (Madon *et al.*, 2015) (Figure 11A). A positive correlation between geothermal gradient and basement depth is indicated by the plot and was used to calculate the estimated geothermal gradient on the basin flanks where there are no data control points. It is noted that, based on the regression line in Figure 11A, in the region outside the basin (where the crust is of "normal" thickness) the geothermal gradient is 41 °C/km. Using the regression equation, control points were obtained outside the data coverage by "predicting" the geothermal gradient based on basement depth derived from the global grids of sediment thickness (GlobSed, Straume *et al*., 2019) and bathymetry (GMRT, Ryan *et al.*, 2009). The resulting contoured map of geothermal gradients is shown in Figure 12. We can see that the Malay Basin is characterised by a zone of high geothermal gradients (>45 °C/km) that extends into the central part of the West Natuna Basin. The Penyu Basin seems to be an area of "average" geothermal gradients (<40 °C/km).

For the areas beyond the deep-water region of Sarawak and Sabah, a different approach was taken to generate control points outside the area of data coverage. It was observed in all the surveys carried out by PETRONAS, Hess, Murphy and JX Nippon in the study area that both geothermal gradient and heat flow are strongly correlated with water depth (bathymetry) (Figure 11B). This behaviour has been observed in studies of other continental margins as well (e.g., Kim *et al*., 2010; Hamamoto *et al.*, 2011; Yamano *et al.*, 2014). Thus, a plot of geothermal gradient and water depth should reveal a strong relationship that can be used to predict the geothermal gradient outside the study area for the purposes of contouring. Hence, the regression line in Figure 11B was used to generate the control points from bathymetry in the region outside of our data coverage. The Global Heat Flow Database also provided some additional datapoints beyond the deep-water areas of North Luconia and Sabah Platform. The resultant map of geothermal gradient for offshore Sarawak and Sabah (Figure 13) shows that the geothermal gradients are higher on the Sarawak Shelf compared to Sabah Shelf but the deep-water areas have the highest geothermal gradients in the area. A zone of high geothermal gradients can be clearly observed on the Sabah Platform (Dangerous Grounds). It should be emphasised, however, that due to the large degree of scatter in geothermal gradient values in the deep-water areas (as shown by the profiles in Figure 9), any apparent trend should be treated with caution.

ESTIMATING HEAT FLOW

From the geothermal gradients we estimated the heat flow and generated heat flow maps for the offshore areas of Malaysia. The vertical heat flow or flux Q at a given location on the Earth's surface is given by (e.g., Allen & Allen, 2013):

$$Q = -k\, dT/dz \quad \ldots\ldots\ldots(1)$$

where dT/dz is the temperature gradient and k is the thermal conductivity of the medium (sediment column).

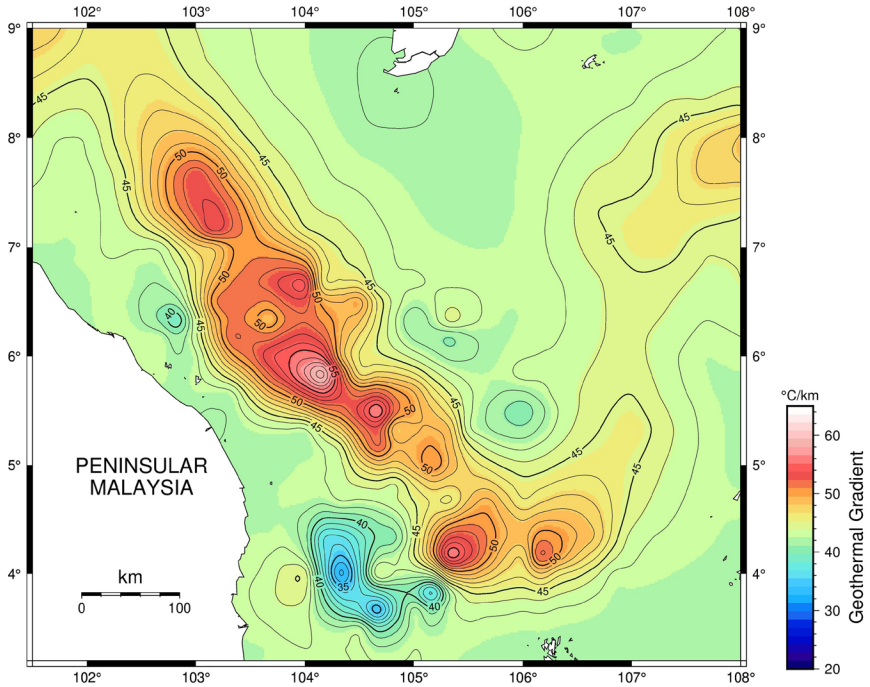

Figure 12: Geothermal gradient map for the Malay and Penyu basins, offshore Peninsular Malaysia. The map was generated from datapoints shown in Figure 4 by interpolation and gridding with continuous curvature with splines (Smith & Wessel, 1990), contoured using a 10-min grid size. "Control" points outside the region of data coverage were generated using the regression equation in Figure 11A in order to minimize contouring artefacts. Data for West Natuna Basin are from the Global Heat Flow Database (GHCG, 2013) and Budi & Miftahul (2014). Contour interval = 5 °C/km.

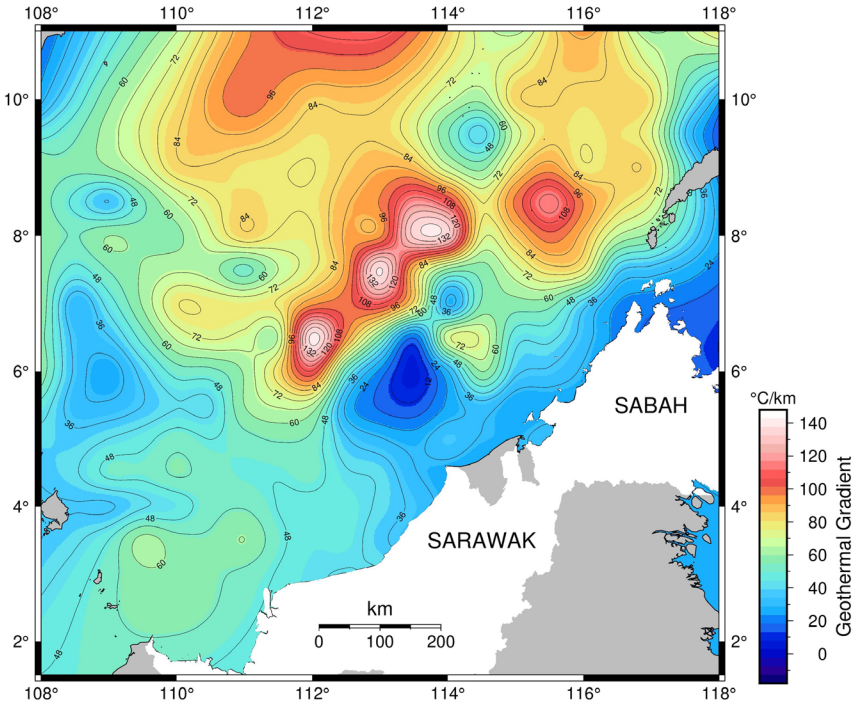

Figure 13: Geothermal gradient map for the Sarawak and Sabah basins, offshore Sarawak and Sabah. This map was generated from data shown in Figure 6 by interpolation and gridding with continuous curvature with splines (Smith & Wessel, 1990), contoured using a 30-min grid size. "Control" points outside the data region, predominantly in the deep-water region of the South China Sea, were generated using the regression equation in Figure 11B, and additional datapoints from the Global Heat Flow Database (GHCG, 2013). Contour interval = 6 °C/km.

The minus sign indicates that the heat flow is in the opposite direction (upward) to the temperature gradient. A fundamental assumption in this analysis is that the heat flow is vertical and constant within the depth range of observation, which is at least down to the well depth over which the BHTs are measured. Similarly, the geothermal gradient is generally assumed as constant throughout the sediment column in the well, which could be as deep as 4000 to 4500 m. The above equation requires a reliable estimate of the thermal conductivity of the sediments penetrated by the wells. In the following section, we review the available thermal conductivity data and outline our approach in deriving heat flow from geothermal gradient.

Thermal conductivity of sediment

In the deep-water areas of the study, the thermal conductivity of seabed sediments is fairly well constrained by the heat flow probe measurements over the length (depth) of the probe instrument, which consists of thermistors attached to a core barrel. In the PETRONAS and other oil company surveys the core barrel was 4 m whereas in the BGR surveys the piston core used was 10 m. The reliability of probe measurements depends on the assumption that there is no disturbance of the substrate when the probe enters the sediment. The average thermal conductivity values of seafloor sediments based on the deep-water surveys range from 0.7 to 0.9 $Wm^{-1}K^{-1}$ (Table 2). In fact, the average thermal conductivity of sea floor sediment (the top 4 m) in the deep-water areas can be quite accurately determined from the regression line between geothermal gradient and heat flow, which is 0.7374 $Wm^{-1}K^{-1}$ (Figure 14).

It is implicitly assumed that the temperature gradient, thermal conductivity and heat flow in the topmost 4 to 10 m of deep-sea sediment represent the entire column of sediment, at least to a depth of few kilometres, comparable to that of a typical oil well drilled on the continental shelf. However, as these values represent only the top 10 m of sediment, which are generally unlithified, they are not necessarily representative of sedimentary section penetrated by oil/gas wells, especially on the continental shelf. It is well-established based on data from International Ocean Drilling Project (ODP and IODP) sites that bulk thermal conductivity of sediment increases with depth due to mechanical and chemical compaction and, consequently, loss of porosity during burial. Figure 15A shows a plot of thermal conductivity of sediments with depth in metres below the sea floor (mbsf) obtained from the report of ODP Leg 184 site 1143 (Shipboard Scientific Party, 2000). This is the closest ODP site to the study area (see Figure 6 for location). According to the report (Shipboard Scientific Party, 2000) the penetrated sediment consists of late Miocene to Quaternary, entirely hemipelagic deposits of fine-grained terrigenous material and calcareous nannofossils with minor occurrences of ash (tuff) layers, turbidite sediments, and green clay layers. Within the depth range of down to about 350 mbsf, there is generally an almost linear relationship between thermal conductivity and depth. As a result of increase in density due to compaction, the thermal conductivity of the sediment increases from about 0.8 $Wm^{-1}K^{-1}$ to as much as 1.2 $Wm^{-1}K^{-1}$. Hence, the average or bulk thermal conductivity of an entire sediment column is also expected to increase as the column depth increases.

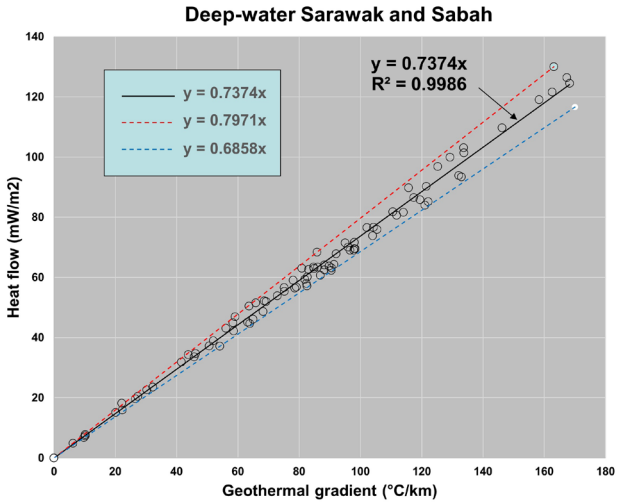

Figure 14: Plot of heat flow vs geothermal gradient at all the marine heat flow stations in the deep-water areas of Sarawak and Sabah (Figure 3). The straight regression line through the points (solid black line) indicates an average thermal conductivity of 0.7374 $Wm^{-1}K^{-1}$. Red and blue dashed lines represent the upper and lower bounds of the data set, with the origin fixed at 0, and correspond to average thermal conductivity of 0.7971 $Wm^{-1}K^{-1}$ and 0.6858 $Wm^{-1}K^{-1}$, respectively. Note that these values represent the thermal conductivity of only the top 4 m of sediment on the deep-sea floor.

In the estimation of heat flow from BHT data in basins on the shelf areas, it is critical to have a reliable estimate of the average or bulk thermal conductivity over the entire sedimentary column penetrated by the wells for which the temperature gradients were calculated. This depth range may be as much as 4500 mbsf, i.e., more than 10 times the length-scale of observation of most ODP holes. Measured thermal conductivity over a depth range of 800 to 2500 m in the Malay Basin from previous works (Wan Ismail, 1984a, b, 1988, 1993; Mohd Firdaus, 1994) are plotted together with the Site 1143 data in Figure 15B. Both datasets lie on the same linear trend, with the thermal conductivity of the Miocene sediments increasing from 2 to 6 $Wm^{-1}K^{-1}$. From this plot, a linear relationship between thermal conductivity and burial depth, as indicated by the regression line, is evident and we have used it to estimate the bulk thermal conductivity of the sediment column.

Estimation of bulk thermal conductivity of sediment

The simplest method to determine heat flow (from equation 1, above) is to assume a single, constant value of thermal conductivity for the entire sediment or rock column at any location in a basin. In the past, for example, an average thermal conductivity of about 1.8 to 1.9 $Wm^{-1}K^{-1}$ has been used (Wan Ismail, 1984a, b, 1993). Surely, the choice

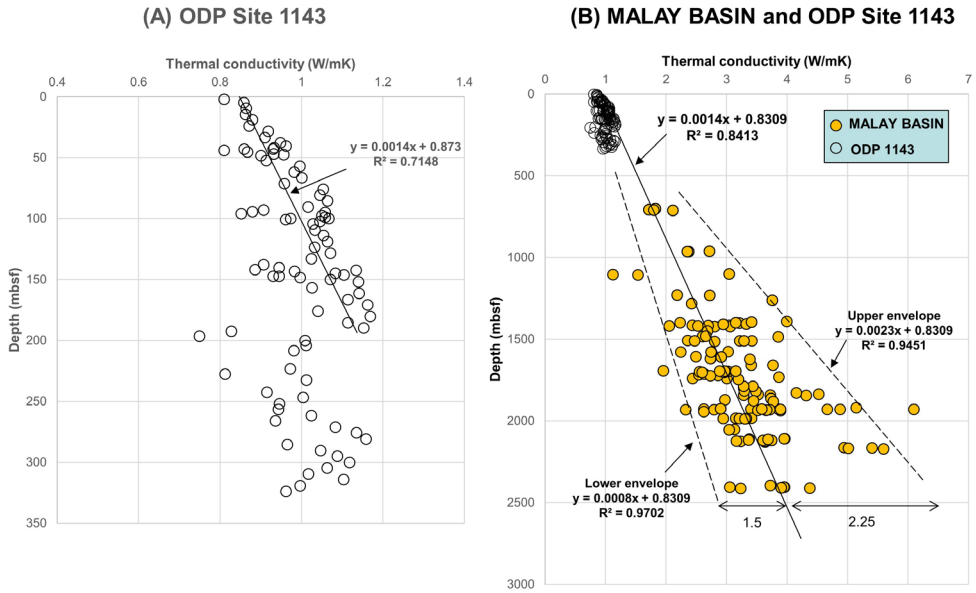

Figure 15: Plot of thermal conductivity of sediments with depth below sea floor (mbsf) (A) at ODP site 1143 (Shipboard Scientific Party, 2000). (B) Measured thermal conductivity of core samples from a depth range of 700 to 2500 m in the Malay Basin (data from Mohd Firdaus, 1994 and Wan Ismail, 1993) plotted with the ODP 1143 data shown in A, which appear as a cluster of points in the top 350 m. A linear regression line through both datasets provides a means to estimate the sediment thermal conductivity at any given depth and derive a bulk thermal conductivity of sediment column to that depth. It is noted that the range of thermal conductivities increases with depth. The root-mean-square (RMS) error, a measure of dispersion of the 276 points from the regression line is 0.5602 $Wm^{-1}K^{-1}$. Regression lines drawn through the lower and upper envelope of points with the origin kept at 0.8309 $Wm^{-1}K^{-1}$ (dashed lines) indicate that the dispersion below and above the average line at 2500 m is 1.5 and 2.25 $Wm^{-1}K^{-1}$, respectively.

of thermal conductivity values has a great impact on the calculated heat flow. Applying a constant thermal conductivity value for the entire basin, however, does not take into account any lateral variation in sediment thermal conductivity due to lithological or facies changes, or the fact that the length-scale of observation (i.e., the depth range of BHT measurements) differs from well to well. Since thermal conductivity increases with depth (Figure 15B), the deeper the well, the higher the bulk thermal conductivity of the sediment column will be. As a result, a constant value of thermal conductivity tends to overestimate the bulk conductivity (and hence, heat flow) in shallow wells while underestimating the bulk conductivity in deep wells. Figure 16 illustrates an example of this problem. Wan Ismail (1993) considered the potential effect of lateral variations in thermal conductivity in the Malay Basin and determined the average thermal conductivity for each well to generate an "average thermal conductivity map". This probably addressed only one part of the problem, which is related to lateral heterogeneities in the sediment, but did not address the variation in bulk thermal conductivity due to the differences in well depth.

The bulk thermal conductivity of sediment down to the depth over which temperature gradients are determined, i.e., from sea floor to the deepest BHT point, can be calculated more accurately based on the last BHT depth or alternatively, if not available, based on the TD of the well, which is generally within 5% of the last BHT depth. The TDs of the 171 wells plotted on the map in Figure 4 range from 1000 to 3930 m, averaging 2367 m. Most of the deeper wells in the Malay Basin (greater than say 2600 m) are located on the basin flanks, particularly in the northeastern area (e.g., the TDs of Bunga Pakma, Bunga Orkid, Bunga Teratai are > 3 km) and some even penetrate the pre-Tertiary basement. Many wells in the Penyu Basin terminate below 2600 m and include older stratigraphic units (seismic Group K and below), and therefore are expected to show relatively higher thermal conductivity than the Malay Basin due to the presence of denser stratigraphic units.

A better approach, therefore, is to estimate the bulk thermal conductivity of the sedimentary column as a function of well depth (TD). This takes into account the increase in sediment thermal conductivity with burial depth. From the plot in Figure 15B, a linear regression equation may be derived as follows:

$$y = 0.0014x + 0.8309 \quad .....(2)$$

This relationship can be used to calculate the thermal conductivity (y) of sediment at any given depth x. The bulk thermal conductivity of the entire sediment column from the sea floor to that depth x is calculated by the harmonic average (Vacquier *et al.*, 1984), given by:

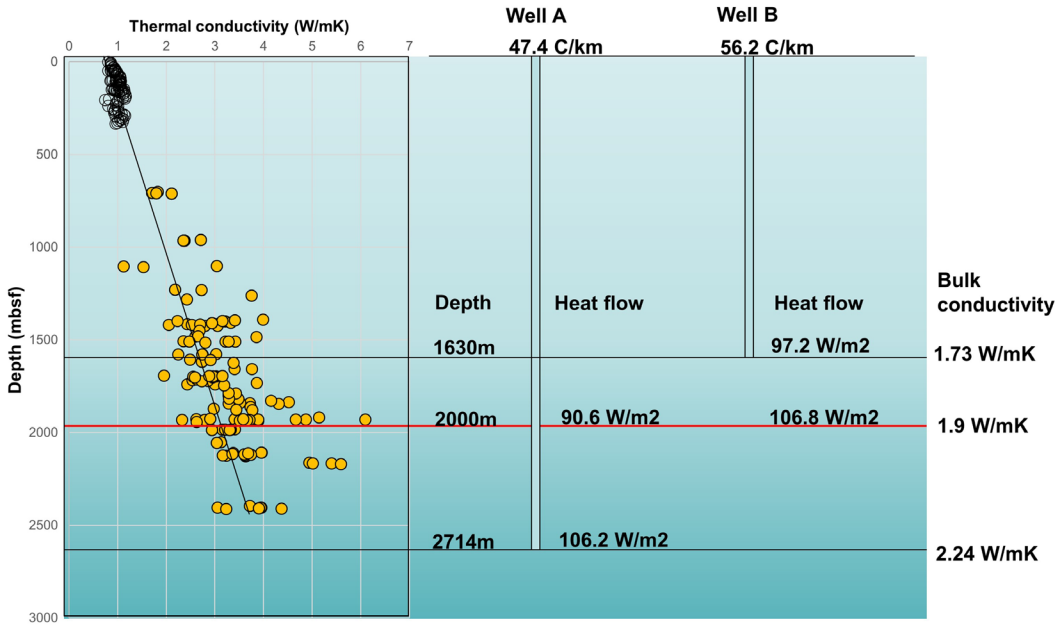

Figure 16: Heat flow calculations in two wells, Well A (Gajah-1, geothermal gradient= 47.4 °C/km) and Well B (Kuda-1, geothermal gradient= 56.2 °C/km) using two approaches: a depth-dependent bulk thermal conductivity model (graph on the left, the same as in Figure 15), and a constant average thermal conductivity of 1.9 $Wm^{-1}K^{-1}$ (red horizontal line). The depth-dependent model gives different bulk thermal conductivities and heat flows that correspond to the respective well depths (TD, black horizontal lines), whereas a constant average thermal conductivity (represented by the red horizontal line) is equivalent to about 2000 m of sediment column in the depth-dependent model. By applying the depth-dependent model, Well A with a TD at 2714 m will have a bulk thermal conductivity of 2.24 $Wm^{-1}K^{-1}$ for the entire sediment column whereas Well B with a TD at 1630 m will have a bulk thermal conductivity of 1.73 $Wm^{-1}K^{-1}$. Thus, applying a constant average conductivity of 1.9 $Wm^{-1}K^{-1}$ will underestimate heat flow at well A and overestimate heat flow at Well B.

$$K = (d1+d2+\ldots dn)/(d1/k1+d2/k2+\ldots dn/kn) \ldots\ldots\ldots(3)$$

where K is the bulk or "effective" thermal conductivity, d1,...dn is the thickness of individual layers of sediment with corresponding thermal conductivities k1,…kn. In this study, k is computed using the regression equation (2) for discrete sediment intervals of 250 m, down to 5000 m. By computing K for each of those sediment layers, a polynomial curve defining the change in bulk thermal conductivity with depth is obtained:

$$K = -3e^{-8}z^2 + 0.0006z + 0.8309 \ldots\ldots\ldots\ldots\ldots\ldots(4)$$

where z is depth at the base of the sediment column (which could be either the last BHT depth or the TD). This equation was used to calculate the bulk thermal conductivity of the well column given the TD, based on which the heat flow was then calculated. The resulting heat flow map for offshore Peninsular Malaysia is shown in Figure 17. Two maps using the different thermal conductivity models are shown: constant thermal conductivity (Figure 17A) and variable or depth-dependent thermal conductivity (Figure 17B). Obviously, by applying a constant thermal conductivity the heat flow map has an almost identical shape to the geothermal gradient map, as it is just a multiplication by the bulk thermal conductivity. On the other hand, the variable thermal conductivity model resulted in a different, probably more geologically realistic, heat flow map that incorporates the lateral variation in bulk thermal conductivities across the basin.

A similar approach was used in calculating heat flow for the areas offshore Sarawak and Sabah. The thermal conductivity curve applied to the Malay Basin (equation 4) may not be applicable to offshore NW Borneo due to different tectonic settings and basin evolution; the Malay Basin being an intracontinental rift whereas the NW Borneo margin are continental margin basins with a complex history of extension and collision. As sediment thermal conductivity is closely linked to porosity and density (Figure 15) and since these basins underwent different burial and diagenetic histories, it would be appropriate to construct a different thermal conductivity curve for offshore Sabah and Sarawak. Unfortunately, measured thermal conductivity data for Sarawak and Sabah, as reported in Mohd Firdaus (1994) (Table 3), are not available. Hence, we constructed a thermal conductivity curve based on data from ODP and IODP drillholes in the South China Sea region, which includes ODP Leg 184, sites 1143-1148 (Wang *et al.*, 2000) and from IODP Expedition 349, sites U1431 and U1433 (Li *et al.*, 2015a, b). The locations of these sites are shown in Figure 18. In addition, due to their extended coring programs which enabled thermal conductivity measurements to be taken down to 2500 mbsf, we also included data from the IODP Expedition 337 Site C0020 in the Shimokita Basin, off Hokaido, northern Japan (Tanikawa *et al.*, 2016) and IODP Expedition 338 Site

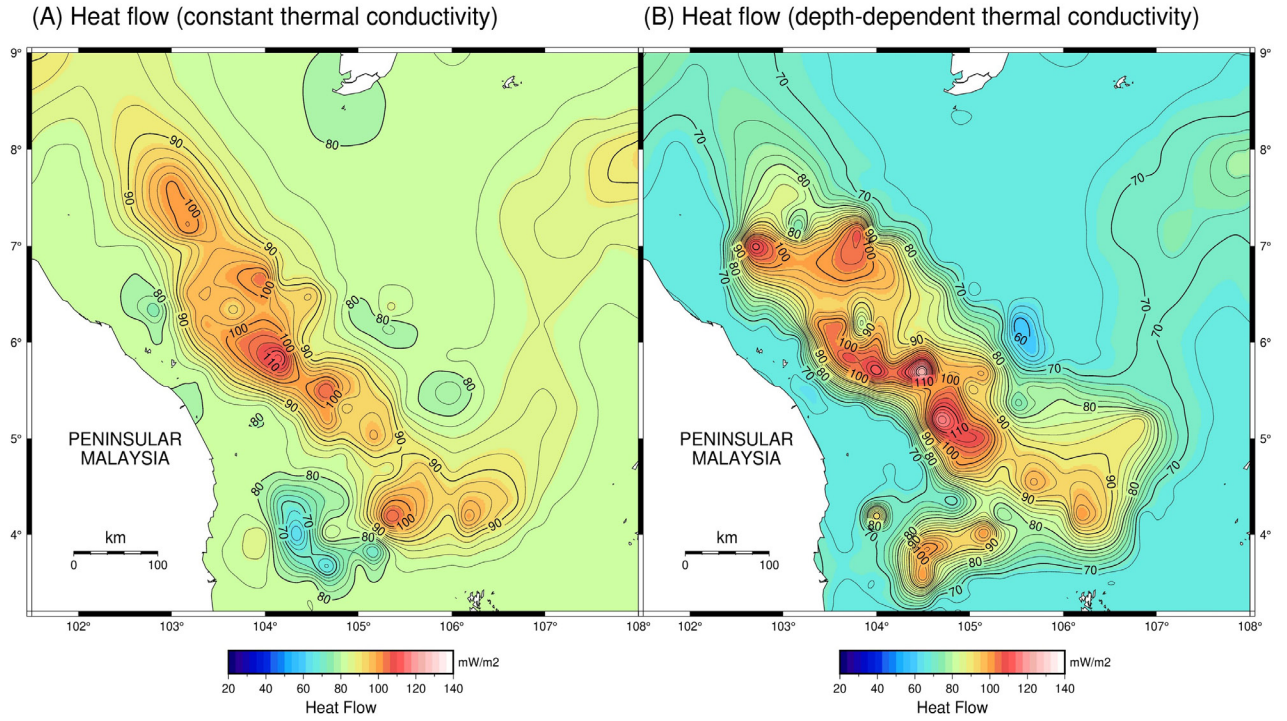

Figure 17: Heat flow maps for offshore Peninsular Malaysia. (A) Using constant thermal conductivity of 1.9 $Wm^{-1}K^{-1}$. (B) Using variable, depth-dependent thermal conductivity model (Figure 15B), as described in the text. The maps were generated by interpolation and gridding with continuous curvature with splines (Smith & Wessel, 1990), contoured at a 10-min grid size. Contour interval = 10 mW/m^2.

Table 3: Thermal parameters for Malaysian sedimentary basins from Mohd Firdaus (1994) and present study.

	Malay Basin, Mohd Firdaus (1994)	Malay Basin (this study)	Sarawak, Mohd Firdaus (1994)	Sarawak (this study)	Sabah, Mohd Firdaus (1994)	Sabah (this study)
Average geothermal gradient (°C/km)	51.8	47	43.3	45	30.5	32
No of wells	101	176	88	319	54	124
Average thermal conductivity ($Wm^{-1}K^{-1}$)	2.95	n.a.	2.34	n.a.	2.35	n.a.
Average heat flow (mW/m^2)	142.9	92	104.3	95	74.0	79

C0002 in the Shikoku Basin, off Kii Peninsula, southern Japan (Sugihara *et al.*, 2014).

All the thermal conductivity data from the ODP and IODP sites mentioned are plotted in Figure 19 to represent a model of sediment thermal conductivity for offshore Sabah and Sarawak (a "NW Borneo Model"). A linear regression equation was obtained from the plot as follows:

$$y = 0.0004x + 1.0447 \quad \text{.....(5)}$$

where y is sediment thermal conductivity and x is depth. From this, we derived a polynomial equation:

$$K = -5e^{-9}z^2 + 0.0002z + 1.0483 \quad \text{.....(6)}$$

that was used to calculate the bulk thermal conductivity K for the sediment column to any given depth z. Based on this approach we generated the heat flow maps for offshore Sarawak and Sabah (Figure 20). We also produced two versions of the map, one applying a constant thermal conductivity (2.34 $Wm^{-1}K^{-1}$) and another using the depth-dependent thermal conductivity model for NW Borneo (Figure 19, equation 6). The two versions look similar but there are significant differences. In particular, there is in both versions the presence of a prominent high heat flow area underlying the Sarawak Shelf, while the high heat flow domain in the deep-water areas have been enhanced by the application of the depth-dependent thermal conductivity model. Additionally, the high heat flows in the Sabah deep-water fold-thrust belt are also enhanced by the depth-dependent thermal conductivity model.

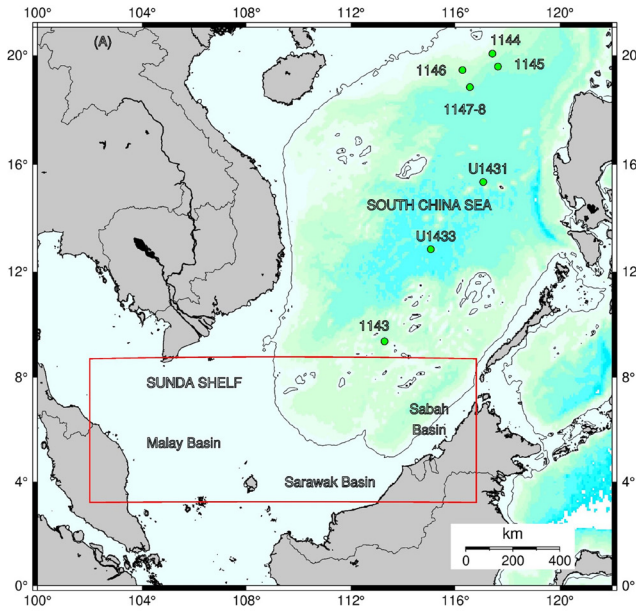

Figure 18: Location of ODP and IODP drill sites in the South China Sea from which thermal conductivity data were obtained and applied to this study. Red rectangle is the study area in this paper.

DISCUSSION

Thermal conductivity model

With this updated compilation of geothermal gradient data, we now have a better data coverage of the offshore regions of Malaysia, in particular the Malay, Sarawak and Sabah basins. Data in the less explored areas such as the Straits of Melaka and eastern Sabah need to be updated as more data become available. From the geothermal gradient data, heat flow maps were derived based on the best-available information on thermal conductivity of the sediments, using either local measurements (as in the Malay Basin) or regional analogues in the South China Sea and similar margins (for Sarawak and Sabah basins) in order to constrain the heat flow estimates. Data from deep-sea drilling projects were used to generate empirical models of thermal conductivity in order to convert geothermal gradient to heat flow. As a result, a more accurate, and probably geologically more realistic, heat flow calculation was achieved by using a varying, depth-dependent model of bulk thermal conductivity instead of a constant value as commonly applied. It is fair to assume that thermal conductivity models are basin-specific, and should be built using local data, due to potentially different facies and burial histories in different basins. This is clearly illustrated in Figure 21 in which the thermal conductivity of sediments in the Nam Con Son and Cuu Long basins, offshore Vietnam, are compared with those of the Malay Basin. The thermal conductivity of sediments in the Vietnamese basins increases

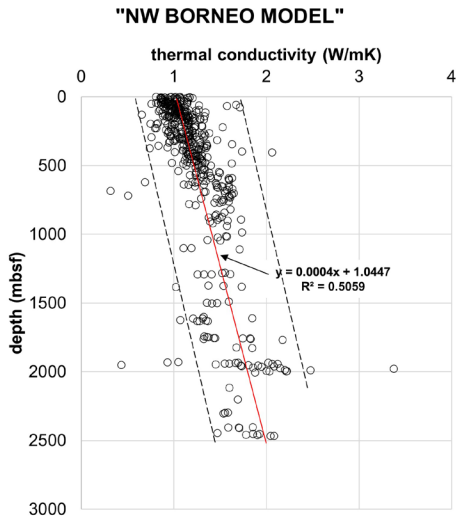

Figure 19: Thermal conductivity data used to derive a thermal conductivity-depth curve for offshore Sarawak and Sabah from ODP and IODP drill sites in the South China Sea: Leg 184 site 1143-1148 (Wang *et al*., 2000), IODP Expedition 349 sites U1431 and U1433 (Li *et al*., 2015a, b) (see locations in Figure 18), with additional data from offshore Japan: IODP Expedition 337 Site C0020 (Tanikawa *et al.*, 2016) and IODP Expedition 338 Site C0002 (Sugihara *et al.*, 2014). There is quite a spread of data above and below the regression line. Ignoring the outermost outlier points above and below the upper and lower envelope lines (shown by dashed lines), the deviation from the regression line is about 0.57 $Wm^{-1}K^{-1}$. The RMS error for the 476 points on this plot is 0.2276 $Wm^{-1}K^{-1}$.

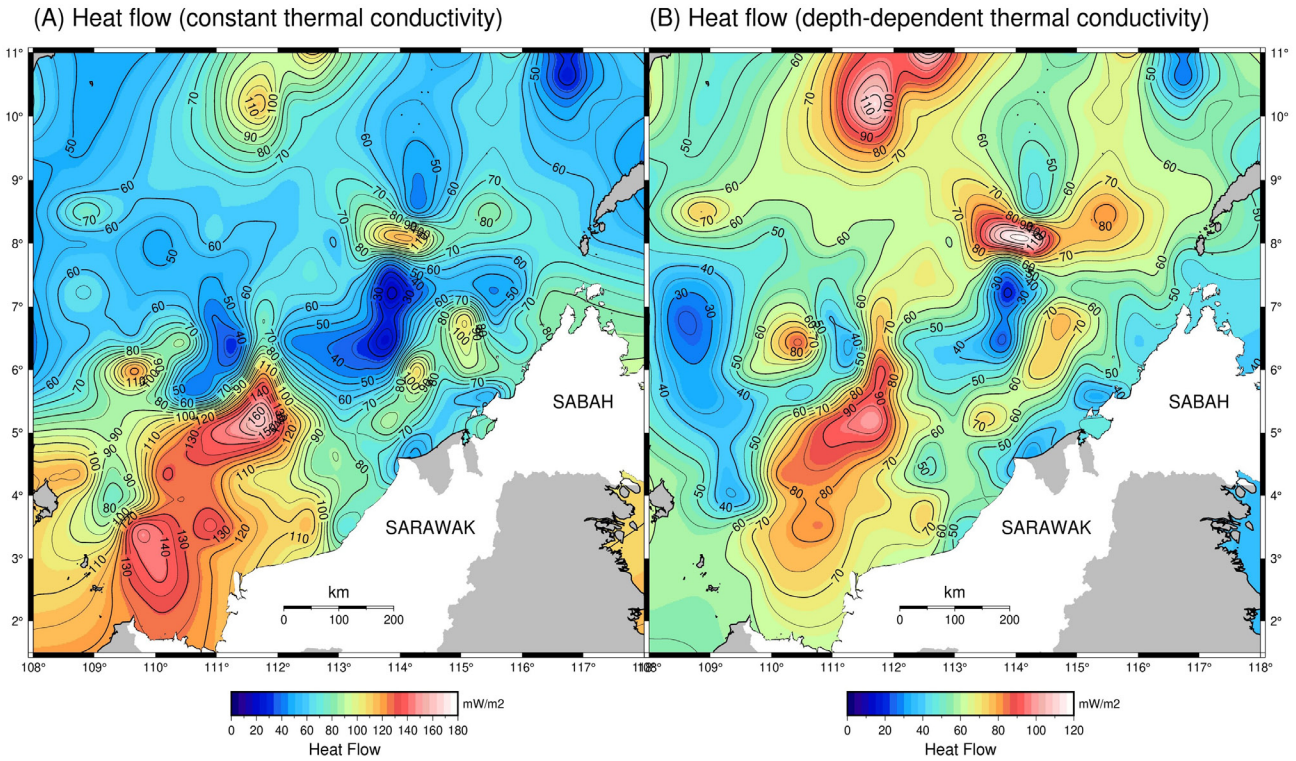

Figure 20: Heat flow maps of offshore Sarawak and Sabah regions. (A) Using a constant bulk thermal conductivity of 2.34 $Wm^{-1}K^{-1}$. (B) Using variable, depth-dependent bulk sediment thermal conductivity model (Figure 19). The maps were generated by interpolation and gridding with continuous curvature with splines (Smith & Wessel, 1990), contoured at a 25-min grid size.

at a much slower rate with burial depth compared to the Malay Basin even though both are located on the Sunda Shelf and underlain by Sundaland continental basement. The higher heat flow in the Malay Basin (average 92 mW/m^2) compared to the Vietnamese basins (70-80 mW/m^2) may have enhanced porosity reduction through diagenetic processes and chemical compaction which influence thermal conductivity.

Heat flow and CO_2 occurrences

Many oil and gas fields in both the Malay and Sarawak basins are associated with high percentage of CO_2 (Idris, 1992; Madon *et al.*, 1999; Mansor *et al.*, 2005; Mansor & Mohd Irwani, 2008). The higher-than-average heat flows observed in both these basins suggest that heat flow may have been a major contributing factor in the occurrences of high-CO_2 gas fields, some of which contain more than

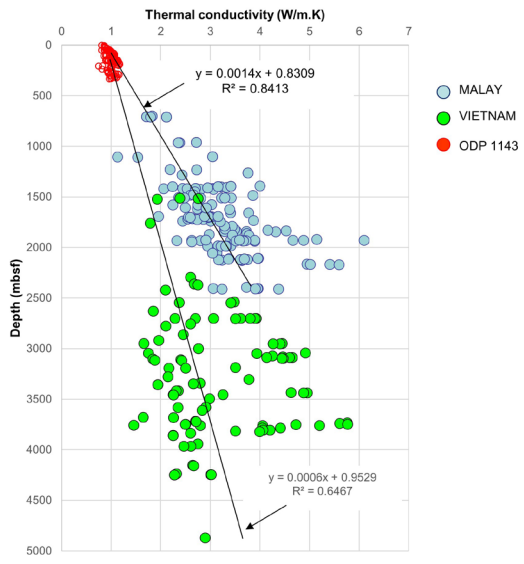

Figure 21: Thermal conductivity of sediments in intracontinental rift basins of the Sunda Shelf, plotted with depth in metres below sea floor (mbsf). Malay Basin data from Wan Ismail (1993) and Mohd Firdaus (1994), same as in Figure 15B. Data from Vietnamese basins, namely Cuu Long and Nam Con Son basins, are from Funnel *et al*. (1997).

75% by volume, such as the K5 field in Sarawak. Studies have shown that a large proportion of the CO_2 in both basins is of inorganic origin, likely to be derived from the metamorphic reactions in carbonate rocks at depth with formation temperatures exceeding 250 °C (Mansor *et al.*, 2005; Mansor & Mohd Irwani, 2008).

Figure 22A is a map of CO_2 distribution in the Sarawak Basin, based on a compilation of data from PETRONAS, and supplemented with data from the neighbouring Sokang and East Natuna basins obtained from SKKMIGAS (2017). The map shows that CO_2 content in the oil and gas pools range from less than 1% to greater than 80% in some fields. While a large proportion of the CO_2 occurrences is in carbonate reef structures in Central Luconia, the volumetrically large occurrences (say, > 20 vol.%) are not found within Central Luconia but primarily to the west of the carbonate province, i.e., over the West Luconia Province and in the Sokang and East Natuna basins (Figure 22B). This may suggest that the lithology of the host-reservoir is not a determining factor in the occurrence of high CO_2, as is expected if the CO_2 sources lie somewhere at depth. An older suite of Tertiary carbonate rocks of Cycle I and Cycle II age is believed to be the primary candidate for the source of the CO_2 (e.g., Madon & Redzuan, 1999; Jong *et al.*, 2003). It is interesting, however, that the zone of high-CO_2 volume is close to the area of highest heat flow on the Sarawak shelf (>70 mW/m^2) (Figure 22C) and appears to overlie the West Luconia Delta depocenter and its northward continuation, the Bunguran Trough, where the basement depth is >10 km (Figure 22D). We speculate that a large proportion of the CO_2 may have been generated from deep sources in the West Luconia Delta and Bunguran Trough and have migrated upwards and laterally into the structures in the neighbouring sub-basins on the fringes of the West Luconia Province. These include the carbonate reefs of Central Luconia and other structural traps in West Luconia, Sokang Basin and East Natuna Basin.

In the Malay Basin the relationship between areas of high CO_2 content and areas of high heat flow is not obvious because the entire basin has a relatively high heat flow. In Figure 23, a map of CO_2 distribution does indicate that areas with the highest CO_2 contents (say >20 vol.%) are concentrated over the central deepest parts of the basin where heat flows are also in the higher range (90-100 mW/m^2), particularly near the Western Hinge Fault Zone (WHFZ). Previous studies have indicated the importance of deep-seated basement faults, including the WHFZ, in the migration of hydrocarbons and other gases from deep sources into the shallower reservoirs (Madon *et al.*, 1999; Mansor & Mohd Irwani, 2008).

CONCLUDING REMARKS

In this study, the geothermal gradient and heat flow database for Malaysia's offshore regions has been significantly improved by the addition of old and new data from unpublished PETRONAS and operator files. We believe this new compilation will be an important contribution to the Global Heat Flow Database. Our new geothermal gradient and heat flow maps for offshore Malaysia may now be compared with maps by other authors (e.g., Shi *et al.*, 2003; Hall & Morley, 2004), and help in regional studies to improve our understanding of the hydrocarbon systems in Malaysia and the surrounding region as a whole.

We have updated the geothermal gradient map of offshore Malaysia with the addition of more than 600 datapoints derived from BHT data in exploration and development wells. An additional 165 points were also added from the deep-water heat flow surveys carried out by PETRONAS and its operating partners up to 2013. From the geothermal gradient data, we generated heat flow maps based on sediment thermal conductivity models derived from both actual measurements of core samples in oil/gas wells and available analogue data from ODP/IODP sites in the wider South China Sea and East Asian region. In our approach, it is suggested that a more accurate and geologically realistic method of calculating heat flow from geothermal gradient can be achieved by determining "effective" bulk sediment conductivity as a function of the depth range of the BHT measurements (essentially, well depth), as opposed to a constant thermal conductivity.

Subsurface geothermal gradient and heat flow information are important in hydrocarbon exploration. Previous studies have demonstrated a correlation between geothermal gradient and oil and gas accumulations, with

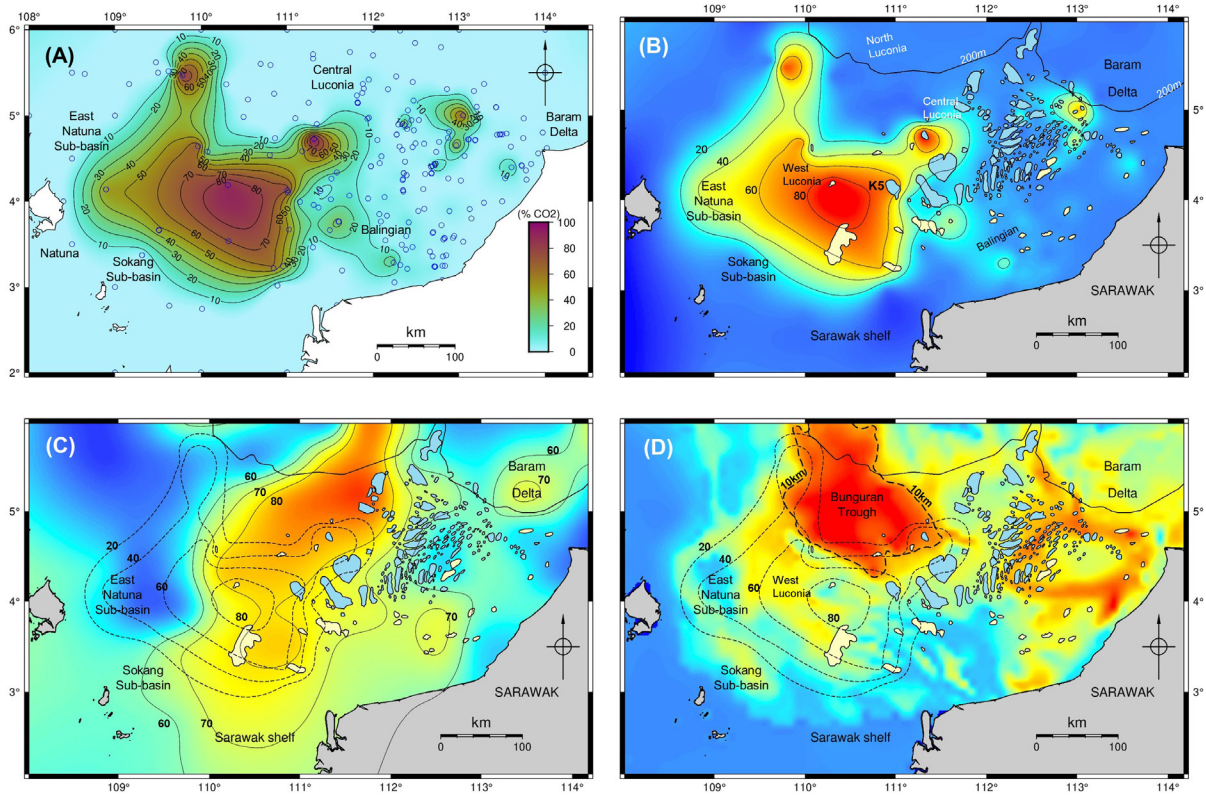

Figure 22: Map of CO_2 distribution in the Sarawak Basin and possible relationships with heat flow. (A) Map of CO_2 distribution (in vol.%) on the Sarawak Basin based on data from PETRONAS (the datapoints shown as blue circles), extended into the neighbouring Sokang and East Natuna sub-basins based on information from SKKMIGAS (2017). (B) Map of CO_2 distribution as in (A) with overlay of oil and gas fields and contours at 20, 40, 60 and 80 vol. %CO_2; warm colours represent high CO_2, cool colours low CO_2. Carbonate reef structures of Central Luconia shown as blue polygons, non-carbonate fields in yellow polygons. Note that the highest percentages of CO_2 are not in Central Luconia but to the west of it in West Luconia and East Natuna and Sokang sub-basins. The 200 m bathymetric contour is also shown for reference. (C) In the same map frame, the CO_2 contours and oil/gas fields are overlaid on heat flow map from Figure 20B, colour shaded to emphasise areas of high heat flow (warm colours) and low heat flows (cool colours). Contours of heat flow at 60, 70 and 80 mW/m^2 are also shown. It is noted that a large part of the high-CO_2 area coincides with the high heat flow area. (D) CO_2 contours over basement depth map of the Sarawak Basin showing the northward continuation of the West Luconia Delta – the Bunguran Trough, outlined by the 10 km contour and straddling the Sarawak Shelf and North Luconia. Basement depth map based on Loftus *et al*. (2003).

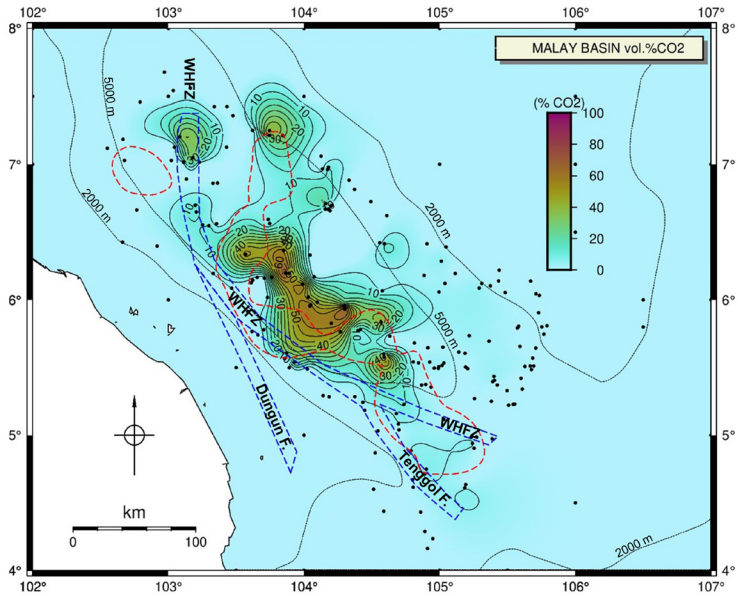

Figure 23: Map of CO_2 distribution in the Malay Basin based on data from PETRONAS (datapoints shown as black dots). The warm-colour shaded areas, with contours at 10% intervals, represent relatively high CO_2 contents. Red dashed lines mark areas with heat flows >100 mW/m^2, based on the map in Figure 17B. Blue dashed lines represent the Western Hinge Fault Zone (WHFZ) and its major splays, Tenggol Fault and Dungun Fault (based on Liew, 1996). The Malay Basin is outlined by sediment isopachs at 2000 m and 5000 m (thin black lines) derived from GlobSed (Straume *et al*., 2019).

gas discoveries generally made in areas of higher heat flow and geothermal gradients (e.g., Jong & Ho, 2000; Bishop, 2002; Madon *et al.*, 2006; Gebregergis & Wan Ismail, 2011). A study of geothermal gradients can help to delineate the temperature regimes and to identify the oil and gas windows in various petroleum provinces, and when superimposed with stratigraphy and structure, the technique provides a useful exploration tool for assessing oil and gas prospects. With the new heat flow maps we have shown a strong correlation between high-CO_2 gas occurrences and high heat flows in the Malay and Sarawak basins.

ACKNOWLEDGEMENTS

We are grateful for the opportunity to review the studies conducted by various operators, including heat flow surveys that have provided useful data and geological insights in our effort to update Malaysia's geothermal gradient and heat flow database and produce the maps presented in this paper. We thank our exploration colleagues in the industry in particular those from Shell and PCSB who continue to supplement our database with more recent well information that allow us to significantly expand the Malaysian geothermal gradient and heat flow database, and we count on their continued support to the project. Our gratitude is also extended to Miss Dayang Aimi Nuraini for drafting of selected figures and to PETRONAS for allowing us to publish the updated geothermal gradient and heat flow maps of Malaysia. Most of the maps in this paper were generated with the public domain software, Generic Mapping Tools (GMT) ver. 6 (Wessel *et al.*, 2019). Last but not least, we would like to thank the three Bulletin reviewers for their constructive comments and suggestions that have helped to improve the manuscript.

REFERENCES

Allen, P.A. & Allen, J.R., 2013. Basin Analysis: Principles and Application to Petroleum Play Assessment. John Wiley & Sons Ltd. 632 p.

Bishop, M.G., 2002. Petroleum system of the Malay Basin province, Malaysia. US Geological Survey, Open-File Report 99-50T, https://pubs.usgs.gov/of/1999/ofr-99-0050/OF99-50T/index.html.

Border, D.P., Blancharde, P.E. & Sharp, Jr., J.M., 1985. Variations in Gulf Coast heat flow created by ground-water flow. AAPG Bulletin, 69(9), 1418.

Brandenburg, A.M., 1994. Temperature and maturity trends of the West Sarawak Shelf: Implications for prospectivity. Shell Exploration Report No. 50744 (unpublished).

Budi, R. Permana & Miftahul, Firdaus, 2014. Temperature profiles and geothermal gradients in Block B West Natuna Basin case study: The impact on Sw calculation for Lower Arang Zone Belut-1 Well. Proc. Indon. Petrol. Assoc., 38th Ann. Conv., 21-23 May, 2014, Jakarta Convention Centre.

Burri, P. & de Miroschedji, A., 1976. Temperature correction methods and application to geothermal studies. NW Borneo, Shell Exploration Report No. 90094 (unpublished).

Cullen, A., 2014. Nature and significance of the West Baram and Tinjar Lines, NW Borneo. Marine and Petroleum Geology, 51, 197-209. http://dx.doi.org/10.1016/j.marpetgeo.2013.11.010.

Evans, T. & Coleman, N., 1974. North Sea geothermal gradients. Nature, 247, 28–30. https://doi.org/10.1038/247028a0.

Franke, D., Barckhausen, U., Heyde, I., Tingay, M. & Ramli, N., 2008. Seismic images of a collision zone offshore NW Sabah/Borneo. Marine and Petroleum Geology, 25, 606-624.

Franke, D., Barckhausen, U., Baristeas, N., Engels, M., Ladage, S., Lutz, R., Montano, J., Pellejera, N., Ramos, E.G. & Schnabel, M., 2011. The continent-ocean transition at the southeastern margin of the South China Sea. Marine and Petroleum Geology, 28, 1187-1204.

Funnell, R., Allis, R. & Huyen, T., 1997. Thermal regimes in two Vietnamese basins, Cuu Long and Nam Con Son, and implications for hydrocarbon generation. Proceedings of an International Conference on Petroleum Systems of SE Asia and Australasia, Indonesian Petroleum Association, 1997, p. 499-509.

Gebregergis, T.M. & Wan Ismail, W. Yusoff, 2011. Burial and thermal history model to evaluate source rock, in Tatau Province, offshore Sarawak Basin. AAPG International Conference and Exhibition, Calgary, Alberta, Canada, September 12-15, AAPG Search and Discovery Article #40706 (2011).

GHCG (Global Heat-Flow Compilation Group), 2013. Component parts of the World Heat Flow Data Collection. PANGAEA, https://doi.org/10.1594/PANGAEA.810104. Accessed 3 January 2021.

Gozzard, S., Kusznir, N., Franke, D., Cullen, A., Reemst, P. & Henstra, A., 2016. South China Sea crustal thickness and oceanic lithosphere distribution from satellite gravity inversion. Petroleum Geoscience, 25, 112–128. https://doi.org/10.1144/petgeo2016-162.

Hall, R. & Morley, C.K., 2004. Sundaland basins. In: Clift, P., Kuhnt, W., Wang, P. & Hayes, D. (Eds.), Continent-Ocean Interactions Within East-Asian Marginal Seas. Geophysical Monograph Series, 49, American Geophysical Union, 55-85. https://doi.org/10.1029/149GM04.

Hall, R. & Breitfeld, H.T., 2017. Nature and demise of the Proto-South China Sea. Bulletin of the Geological Society of Malaysia, 63, 61–76.

Hamamoto, H., Yamano, M., Goto, S., Kinoshita, M., Fujino, K. & Wang, K., 2011. Heat flow distribution and thermal structure of the Nankai subduction zone off the Kii Peninsula. Geochemistry, Geophysics, Geosystems, 12, Q0AD20. https://doi.org/10.1029/2011GC003623.

Hayes, D.E. & Nissen, S.S., 2005. The South China sea margins: Implications for rifting contrasts. Earth and Planetary Science Letters, 237, 601-616. https://doi.org/10.1016/j.epsl.2005.06.017.

Hazebroek, H.P. & Tan, D.N.K., 1993. Tertiary evolution of the NW Sabah continental margin. Bulletin of the Geological Society of Malaysia, 33, 195-210.

Hermanrud, C., Cao, S. & Lerche, I, 1990. Estimates of virgin rock temperature derived from BHT measurements: bias and error. Geophysics, 55, 924-931. https://doi.org/10.1190/1.14429081991.

Hermanrud, C., Lerche, I. & Meisingset, K.K., 1991. Determination of virgin rock temperature from drillstem tests. Journal of Petroleum Technology, 43(9), 1126-1131.

Hinz, K., Fritsch, J., Kempter, E.H.K., Mohammad, A.M., Vosberg,

H., Weber, J. & Benavidez, J., 1989. Thrust tectonics along the northwestern continental margin of Sabah/Borneo. Geologische Rundschau, 78(3), 705-730.

Hutchison, C.S., 2004. Marginal basin evolution: the southern South China Sea. Marine and Petroleum Geology, 21, 1129–1148.

Hutchison, C.S., 2010. The North-West Borneo trough. Marine Geology, 271, 32–43.

Hutchison, C.S. & Vijayan, V.R., 2010. What are the Spratlys? Journal of Asian Earth Sciences, 39, 371-385.

Idris, M.B., 1992. CO_2 and N_2 contamination in J32-1, SW Luconia, offshore Sarawak. Bulletin of the Geological Society of Malaysia, 32, 239-246.

Iyer, S., 2019. Sarawak Basin: tectono-stratigraphic provinces and their seismic expressions. In: Geophysical Applications in Malaysian Basins. PETRONAS, Kuala Lumpur, 105-133.

Jabbar, S.F., Amin Suyitno, D.S., Azwa Jannah, A.B., Khairul Amri, B., Basiron, J., Ayub, A. & Madon, M., 2015. The NNG Discovery: A new oil play in the pre-Cycle I basement, onshore Sarawak. Asia Petroleum Geoscience and Exhibition (APGCE) 2015, 12-13 October, Kuala Lumpur. Proceedings and Abstracts.

Jones, F.W. & Majorowicz, J.A., 1987. Some aspects of the thermal regime and hydrodynamics of the western Canadian sedimentary basin. Geological Society London Special Publications, 34, 79-85. https://doi.org/10.1144/GSL.SP.1987.034.01.06.

Jong, J. & Ho, F., 2000. A regional overview of the NW Borneo margin. Shell Exploration Report No. 51121 (unpublished).

Jong, J., Wang, H.D. & BeMent, W.O., 2003. A study of distribution and possible origins of CO_2 in offshore Sarawak, Malaysia. Shell EP Newsletter, Article EP 2003-7320.

Karner, G., 1991. Sediment blanketing and the flexural strength of extended continental lithosphere. Basin Research, 3, 177-185. https://doi.org/10.1111/j.1365-2117.1991.tb00127.x.

Kenyon, C.S. & Beddoes, L.R., 1977. Geothermal Gradient Map of Southeast Asia, South East Asia Petroleum Exploration Society and Indonesian Petroleum Association, 1977. 50 p.

Kessler, F.L. & Jong, J., 2016. The West Baram Line in the southern South China Sea: a discussion with late Prof. H.D. Tjia on its possible onshore continuation and nomenclature. Warta Geologi, 42(3/4), 84-87.

Kim, Y., Huh, M. & Lee, E.Y., 2020. Numerical modelling to evaluate sedimentation effects on heat flow and subsidence during continental rifting. Geosciences, 10, 451.dhttp://dx.doi.org/10.3390/geosciences10110451.

Kim, Y.-G., Lee, S.-M. & Matsubayashi, O., 2010. New heat flow measurements in the Ulleung Basin, East Sea (Sea of Japan): Relationship to local BSR depth, and implications for regional heat flow distribution. Geo-Marine Letters. https://doi.org/10.1007/s00367-010-0207-x.

Lee, C., 2000. Regional Seismic Horizon Offshore West Sabah. Shell Exploration Report No. 70619 (unpublished).

Li, C.-F., Lin, J., Kulhanek, D.K., Williams, T., Bao, R., Briais, A., Brown, E.A., Chen, Y., Clift, P.D., Colwell, F.S., Dadd, K.A., Ding, W., Hernández-Almeida, I., Huang, X.-L., Hyun, S., Jiang, T., Koppers, A.A.P., Li, Q., Liu, C., Liu, Q., Liu, Z., Nagai, R.H., Peleo-Alampay, A., Su, X., Sun, Z., Tejada, M.L.G., Trinh, H.S., Yeh, Y.-C., Zhang, C., Zhang, F., Zhang, G.-L., & Zhao, X., 2015a. Site U1431. In: Li, C.-F., Lin, J., Kulhanek, D.K., and the Expedition 349 Scientists (Eds.), Proceedings of the International Ocean Discovery Program, 349: South China Sea Tectonics: College Station, TX (International Ocean Discovery Program). http://dx.doi.org/10.14379/iodp.proc.349.103.2015.

Li, C.-F., Lin, J., Kulhanek, D.K., Williams, T., Bao, R., Briais, A., Brown, E.A., Chen, Y., Clift, P.D., Colwell, F.S., Dadd, K.A., Ding, W.-W., Hernández-Almeida, I., Huang, X.-L., Hyun, S., Jiang, T., Koppers, A.A.P., Li, Q., Liu, C., Liu, Q., Liu, Z., Nagai, R.H., Peleo-Alampay, A., Su, X., Sun, Z., Tejada, M.L.G., Trinh, H.S., Yeh, Y.-C., Zhang, C., Zhang, F., Zhang, G.-L. & Zhao, X., 2015b. Site U1433. In: Li, C.-F., Lin, J., Kulhanek, D.K., and the Expedition 349 Scientists (Eds.), Proceedings of the International Ocean Discovery Program, 349: South China Sea Tectonics: College Station, TX (International Ocean Discovery Program). http://dx.doi.org/10.14379/iodp.proc.349.105.2015.

Liew, K.K., 1996. Structural history of hinge fault system of the Malay Basin. Bulletin of the Geological Society of Malaysia, 39, 33-50.

Loftus, G.W.F., Jong, J., Boer, L., Hiser, D.W., Hong, M., Sankosik, H., Wang, H.D. & Wee, G., 2003. NW Borneo Shelf Basin Framework Study. Unpublished Shell Report EP 2003 3166).

Madon, M., 1999. Basin types, tectono-stratigraphic provinces, and structural styles. In: PETRONAS "The Petroleum Geology and Resources of Malaysia", Chapter 6, 77-111.

Madon, M. & Watts, A.B., 1998. Gravity anomalies, subsidence history, and the tectonic evolution of the Malay and Penyu Basins. Basin Research, 10, 375-392.

Madon, M. & Redzuan, Abu Hassan, 1999. Tatau Province. In: PETRONAS "The Petroleum Geology and Resources of Malaysia", Chapter 17, 411-426.

Madon, M., Abolins, P., Mohammad Jamaal Hoesni & Mansor Ahmad, 1999. Malay Basin. In PETRONAS "The Petroleum Geology and Resources of Malaysia", Chapter 8, 171-218.

Madon, M., Jiu-Shan Yang, Abolins, P., Redzuan Abu Hassan, Azmi M. Yakzan & Saiful Bahari Zainal, 2006. Petroleum systems of the Northern Malay Basin. Bulletin of the Geological Society of Malaysia, 49, 125-134.

Madon, M., Cheng Ly Kim & Wong, R., 2013. The structure and stratigraphy of deepwater Sarawak, Malaysia: implications for tectonic evolution. Journal of Asian Earth Sciences, 76, 312-333. https://doi.org/10.1016/j.jseaes.2013.04.040.

Madon, M., Liu, J., Ayub, A., Hamdan, M. & Azhar, Y., 2015. Fractured basement play in the Malay Basin: Play concept and seismic recognition. Asia Petroleum Geoscience and Exhibition (APGCE) 2015, 12-13 October, Kuala Lumpur. Proceedings and Abstracts.

Madon, M., Jong, J., Kessler, F.L., Murphy, C., Your, L., Mursyidah A. Hamid & Nurfadhila M. Sharef, 2019. Overview of the structural framework and hydrocarbon plays in the Penyu Basin, offshore Peninsular Malaysia. Bulletin of the Geological Society of Malaysia, 68, 1-23. https://doi.org/10.7186/bgsm68201901.

Majorowicz, J.A., Linville, L. & Osadetz, K.G., 1986. The relationship of hydrocarbon occurrences to geothermal gradients and time-temperature indices in Mesozoic formations of southern Alberta. Bulletin of Canadian Petroleum Geology, 34, 226-239.

Mansor, Ahmad & Mohd Irwani, Saidi, 2008. Carbon dioxide (CO_2) distribution in the Sarawak Basin, and its relationship with entrapment. PGCE 2008, Kuala Lumpur.

Mansor Ahmad, Norhafizah Mohamed & Nakayama, K., 2005. Carbon dioxide (CO_2) distribution in the Malay Basin, Malaysia. PGCE 2005, Kuala Lumpur.

Matsubayashi, O. & Uyeda, S., 1979. Estimation of heat flow in

certain exploration wells in offshore areas of Malaysia. Bulletin of the Earthquake Research Institute, 54, 31-44.

McGiveron, S. & Jong, J., 2018. Complex geothermal gradients and their implications, deepwater Sabah, Malaysia. Bulletin of the Geological Society of Malaysia, 66, 15 – 22. http://dx.doi.org/10.7186/bgsm66201803.

Mohd Firdaus, Abdul Halim, 1994. Geothermics of the Malaysian sedimentary basins. Bulletin of the Geological Society of Malaysia, 36, 163-174.

Morley, C.K., 2002. A tectonic model for the Tertiary evolution of strike-slip faults and rift basins in SE Asia. Tectonophysics, 347, 189-215.

Morley, C.K. & Leong, L.C., 2008. Evolution of deep-water synkinematic sedimentation in a piggyback basin, determined from three-dimensional seismic reflection data. Geosphere 4(6). https://doi.org/10.1130/GES00148.1.

Nagihara, S., Brooks, J.M., Cole, G. & Lewis, T., 2002. Application of marine heat flow data important in oil, gas exploration. Oil and Gas Journal, July 2002.

Peters, K. & Nelson, P.H., 2009. Criteria to determine borehole formation temperatures for calibration of basin and petroleum system models. Search and Discovery Article #40463 (2009). AAPG Annual Convention and Exhibition, Denver, Colorado, USA, June 7-10, 2009. Posted November 10, 2009.

Pubellier, M. & C.K. Morley, 2014. The basins of Sundaland (SE Asia): Evolution and boundary conditions. Marine and Petroleum Geology, 58, Part B, 555-578. https://doi.org/10.1016/j.marpetgeo.2013.11.019.

Rutherford, K.J. & M.K. Qureshi, 1981. Geothermal gradient map of Southeast Asia 2nd edition. South East Asia Petroleum Exploration Society and Indonesian Petroleum Association. 51 p.

Rice-Oxley, E., 1992. Regional stratigraphy of the Sarawak Shelf. Shell Exploration Report No. 03-0889 (unpublished).

Ryan, W.B.F., S.M. Carbotte, J.O. Coplan, S. O'Hara, A. Melkonian, R. Arko, R.A. Weissel, V. Ferrini, A. Goodwillie, F. Nitsche, J. Bonczkowski, & R. Zemsky, 2009. Global Multi-Resolution Topography synthesis, Geochem. Geophys. Geosyst., 10, Q03014. http://dx.doi.org/10.1029/2008GC002332.

Sandal, S.T., 1997. The geology and hydrocarbon resources of Negara Brunei Darussalam – Brunei Shell Petroleum Company and Brunei Museum, Syabas, 2nd Edition. 243 p.

Savva, D., Pubellier, M., Franke, D., Chamot-Rooke, N., Meresse, F., Steuer, S. & Auxietre, J.L., 2014. Different expressions of rifting on the South China Sea margins. Marine and Petroleum Geology, 58, 579-598. https://doi.org/10.1016/j.marpetgeo.2014.05.023.

Scherer, M., Jong, J., Sha, L.P. & Godeng, F., 2000. West Baram Delta study – A regional study of the hydrocarbon habitat, Shell Exploration Report No. 51100 (unpublished).

Shi, X., Qiu, X., Xia, K. & Zhou, D., 2003. Characteristics of surface heat flow in the South China Sea. Journal of Asian Earth Sciences, 22, 265–277.

Shipboard Scientific Party, 2000. 4. Site 1143. In: Wang, P., Prell, W.L., Blum, P. *et al.* (Eds.), Proceedings of the Ocean Drilling Program, Initial Reports Volume 184, p. 68. https://doi.org/10.2973/odp.proc.ir.184.2000. Available at http://www-odp.tamu.edu/publications/184_IR/chap_04/chap_04.htm, last accessed 21 January 2021.

SKKMIGAS, 2017. Status Migas di Natuna. Divisi Perencanaan Eksplorasi Deputi Perencanaan, SKKMIGAS, 16 p. (document GSM_11_Natuna_(SKK_Migas).pdf, https://psg.bgl.esdm.go.id/informasi/pusat-unduhan/doc_download/175-status-migas-di-natuna, last accessed 31 March 2021.

Smith, W. H. F. & P. Wessel, 1990. Gridding with continuous curvature splines in tension. Geophysics, 55(3), 293–305. https://doi.org/10.1190/1.1442837.

Straume, E.O., Gaina, C., Medvedev, S., Hochmuth, K., Gohl, K., Whittaker, J. M., Abdul Fattah, R., Doornenbal, J.C. & Hopper, J.R., 2019. GlobSed: Updated total sediment thickness in the world's oceans. Geochemistry, Geophysics, Geosystems, 20, 1756-1772. doi: 10.1029/2018GC008115.

Sugihara, T., Kinoshita, M., Araki, E., Kimura, T., Kyo, M., Namba, Y., Kido, Y., Sanada, Y. & Moe Kyaw Thu, 2014. Re-evaluation of temperature at the updip limit of locked portion of Nankai megasplay inferred from IODP Site C0002 temperature observatory. Earth, Planet and Space, 66, 107. https://doi.org/10.1186/1880-5981-66-107.

Tang, X-Y., Hu, S-B., Zhang, G-C., Liang, J-S., Yang, S-C., Rao, S. & Li, W-W., 2014. Geothermal characteristics and hydrocarbon accumulation of the northern marginal basins, South China Sea. Chinese Journal of Geophysics, 57(1), 64-78.

Tanikawa, W., Tadai, O., Morita, S., Lin, W., Yamada, Y., Sanada, Y., Moe, K., Kubo, Y. & Inagaki, F., 2016. Thermal properties and thermal structure in the deepwater coalbed basin off the Shimokita Peninsula, Japan. Marine and Petroleum Geology, 73, 445-461. http://dx.doi.org/10.1016/j.marpetgeo.2016.03.006.

Taylor, B. & D. E. Hayes, 1983. Origin and history of the South China Sea Basin. In: D. E. Hyes (Ed.), The tectonic and geological evolution of the south east Asian seas and islands, part II. American Geophysical Union Geophysical Monograph Series, 27, 23-56.

Vacquier, V., Mathieu, Y., Legrende, E. & Blondin, E., 1984. Experiment on estimating thermal conductivity of sedimentary rocks from oil well logging. American Association of Petroleum Geologists Bulletin, 72(6), 758-764.

Wan Ismail, Wan Yusoff, 1984a. Heat flow study in the Malay Basin. CCOP Technical Publ., 15, 77-87.

Wan Ismail, Wan Yusoff, 1984b. Heat flow study in the Malay basin. Combined Proceedings of the Joint Ascope/CCOP Workshops on Heat Flow, ASCOPE/TP 5, CCOP /TP 15.

Wan Ismail, Wan Yusoff, 1988. Heat flow in offshore Malaysian basins. Proceedings of the CCOP Heat Flow Workshop III CCOP /TP 21, 39-54.

Wan Ismail, Wan Yusoff, 1990. Heat flow in offshore Malaysian basins. CCOP Technical Publ., 21, 39-54.

Wan Ismail, Wan Yusoff, 1993. Geothermics of the Malay Basin, Offshore Malaysia. Durham University, MSc Thesis (unpublished).

Wang, P., Prell, W.L., Blum, P. & Shipboard Scientific Party, 2000. Proceedings of the Ocean Drilling Program, Initial Reports Volume 184. ISSN 1096-2158, https://doi.org/10.2973/odp.proc.ir.184.2000.

Waples, D.W. & Mahadir, Ramly, 1994. A simple statistical method for correcting and standardizing heat flows and subsurface temperatures derived from log test data. Bulletin of the Geological Society of Malaysia, 37, 253-267.

Waples, D.W. & Mahadir, Ramly, 2001. A statistical method for correcting log-derived temperatures. Petroleum Geoscience, 7, 231-240.

Wessel, P., Luis, J. F., Uieda, L., Scharroo, R., Wobbe, F., Smith, W. H. F., & Tian, D., 2019. The Generic Mapping Tools version

6. Geochemistry, Geophysics, Geosystems, 20, 5556–5564. https://doi.org/10.1029/2019GC008515.

Yamano, M., Kawada, Y. & Hamamoto, H., 2014. Heat flow survey in the vicinity of the branches of the megasplay fault in the Nankai accretionary prism. Earth Planet Sp 66, 126. https://doi.org/10.1186/1880-5981-66-126.

Yan, P. & Liu, H., 2004. Tectonic-stratigraphic division and blind fold structures in Nansha Waters, South China Sea. Journal of Asian Earth Sciences, 24, 337-348.

Yu, Sheng Mo & Yap, Kok Thye, 2019. Malay and Penyu basins: seismic stratigraphy and structural styles. In: Geophysical Applications in Malaysian Basins. PETRONAS, Kuala Lumpur, 51-68.

Zielinski, G.W. & Zielinski, L.B., 2003. Heatflow measurements over Sarawak and Sabah deep water area. Surface Geochemical Services AS, Report for Petronas, PRSS-11-03-32. 33 p.

Zielinski, G.W., Bjorøy, M., Zielinski, R.L.B. & Ferriday, I.L., 2007. Heat flow and surface hydrocarbons on the Brunei continental margin. American Association of Petroleum Geologists Bulletin, 91(7), 1053–1080.

Manuscript received 17 February 2021
Revised manuscript received 2 April 2021
Manuscript accepted 5 April 2021